

2020

Bone Morphogenic Proteins are Immunoregulatory Cytokines Controlling FOXP3⁺ T_{reg} Cells

Lauren M. Browning
Old Dominion University

Caroline Miller
Old Dominion University, cmill012@odu.edu

Michal Kuczma

Maciej Pietrzak

Yu Jing
Old Dominion University, yjing@odu.edu

See next page for additional authors

Follow this and additional works at: https://digitalcommons.odu.edu/bioelectrics_pubs



Part of the [Biology Commons](#), and the [Cell Anatomy Commons](#)

Original Publication Citation

Browning, L. M., Miller, C., Kuczma, M., Pietrzak, M., Jing, Y., Rempala, G., Muranski, P., Ignatowicz, L., & Kraj, P. (2020). Bone morphogenic proteins are immunoregulatory cytokines controlling FOXP3⁺ T_{reg} Cells. *Cell reports*, 33(1), 24 pp., Article 108219. <https://doi.org/10.1016/j.celrep.2020.108219>

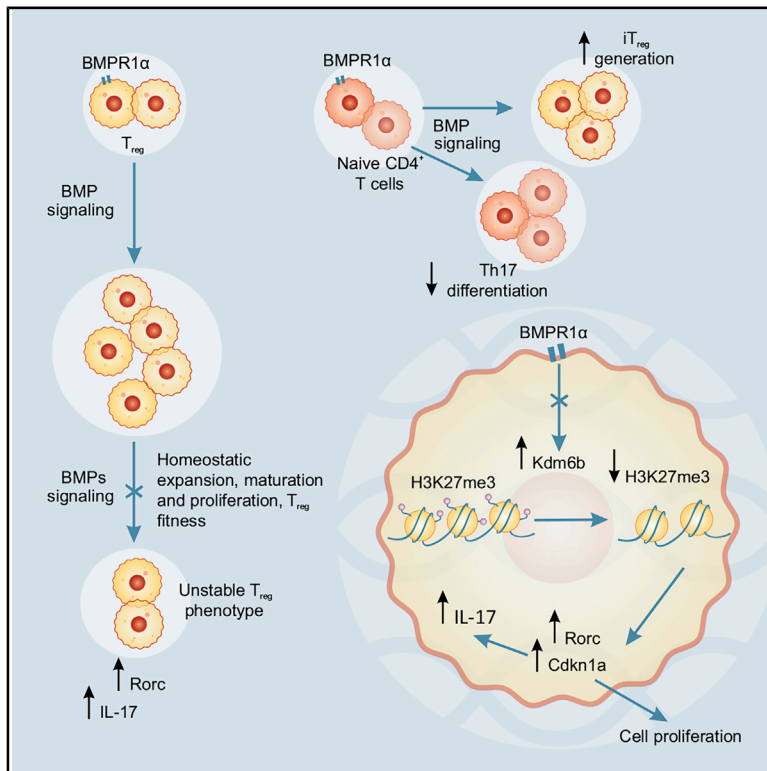
This Article is brought to you for free and open access by the Frank Reidy Research Center for Bioelectrics at ODU Digital Commons. It has been accepted for inclusion in Bioelectrics Publications by an authorized administrator of ODU Digital Commons. For more information, please contact digitalcommons@odu.edu.

Authors

Lauren M. Browning, Caroline Miller, Michal Kuczma, Maciej Pietrzak, Yu Jing, Grzegorz Rempala, Pawel Muranski, Leszek Ignatowicz, and Piotr Kraj

Bone Morphogenic Proteins Are Immunoregulatory Cytokines Controlling FOXP3⁺ T_{reg} Cells

Graphical Abstract



Authors

Lauren M. Browning, Caroline Miller, Michal Kuczma, ..., Pawel Muranski, Leszek Ignatowicz, Piotr Kraj

Correspondence

pkraj@odu.edu

In Brief

Browning et al. find that bone morphogenic proteins, cytokines controlling tissue differentiation and homeostasis, have an immunoregulatory function when signaling through BMPR1 α expressed by Th and T_{reg} cells. BMPR1 α sustains the phenotype and stability of T_{reg} cells and controls the generation of effector Th cells modulating the activity of chromatin modifier KDM6B demethylase.

Highlights

- BMPR1 α mediates immunomodulatory functions of bone morphogenic proteins
- BMPR1 α signaling controls the phenotype and stability of peripheral T_{reg} cells
- Chromatin modifications mediated by KDM6B are associated with BMPR1 α signaling



Article

Bone Morphogenic Proteins Are Immunoregulatory Cytokines Controlling FOXP3⁺ T_{reg} Cells

Lauren M. Browning,¹ Caroline Miller,¹ Michal Kuczma,² Maciej Pietrzak,³ Yu Jing,⁴ Grzegorz Rempala,⁵ Pawel Muranski,⁶ Leszek Ignatowicz,² and Piotr Kraj^{1,7,*}

¹Department of Biological Sciences, Old Dominion University, Norfolk, VA 23529, USA

²Institute for Biomedical Sciences, Georgia State University, Atlanta, GA 30303, USA

³Department of Biomedical Informatics, Ohio State University, Columbus, OH 43210, USA

⁴Center for Bioelectrics, Old Dominion University, Norfolk, VA 23529, USA

⁵College of Public Health, Ohio State University, Columbus, OH 43210, USA

⁶Columbia University Medical Center, New York, NY 10032, USA

⁷Lead Contact

*Correspondence: pkraj@odu.edu

<https://doi.org/10.1016/j.celrep.2020.108219>

SUMMARY

Bone morphogenic proteins (BMPs) are members of the transforming growth factor β (TGF- β) cytokine family promoting differentiation, homeostasis, and self-renewal of multiple tissues. We show that signaling through the bone morphogenic protein receptor 1 α (BMPR1 α) sustains expression of FOXP3 in T_{reg} cells in peripheral lymphoid tissues. BMPR1 α signaling promotes molecular circuits supporting acquisition and preservation of T_{reg} cell phenotype and inhibiting differentiation of pro-inflammatory effector Th1/Th17 CD4⁺ T cell. Mechanistically, increased expression of KDM6B (JMJD3) histone demethylase, an antagonist of the polycomb repressive complex 2, underlies lineage-specific changes of T cell phenotypes associated with abrogation of BMPR1 α signaling. These results reveal that BMPs are immunoregulatory cytokines mediating maturation and stability of peripheral FOXP3⁺ regulatory T cells (T_{reg} cells) and controlling generation of iT_{reg} cells. Thus, we establish that BMPs, a large cytokine family, are an essential link between stromal tissues and the adaptive immune system involved in sustaining tissue homeostasis by promoting immunological tolerance.

INTRODUCTION

Regulatory T cells (T_{reg}) expressing transcription factor FOXP3 are essential for maintaining immune system homeostasis (Josefowicz et al., 2012; Sakaguchi et al., 2010). A decreased proportion or dysregulation of T_{reg} cells precipitates uncontrolled immune activation and is a cause of autoimmune diseases. However, compromised homeostatic function of T_{reg} cells is not always associated with their reduced frequency or altered phenotype (Kuchroo et al., 2012; Long and Buckner, 2011). Abrogating cytokine signaling, altered function of molecules impacting FOXP3 protein stability or modifications of chromatin proteins associated with the FOXP3 gene locus, which define its epigenetic status, often underlie T_{reg} cell deficiency and inability to control inflammation in specific anatomic locations (Bettini et al., 2012; Do et al., 2017; Konkel et al., 2017; Min, 2017; Wan and Flavell, 2007; Wing et al., 2019). Heterogeneity of the T_{reg} cell population may account for differential stability of FOXP3 expression (Sawant and Vignali, 2014; Weinmann, 2014). In peripheral lymphoid organs, thymus-derived T_{reg} (tT_{reg}) cells are complemented by peripherally induced T_{reg} cells (pT_{reg}) generated from CD4⁺ Th cells in response to stimulation with self

or non-self antigens (Abbas et al., 2013; Kendal et al., 2011; Lathrop et al., 2011; Martin et al., 2013). tT_{reg} and pT_{reg} cells have some nonoverlapping suppressor functions, and both are necessary to control inflammation (Bilate and Lafaille, 2012; Cobbold et al., 2004; Curotto de Lafaille et al., 2008; Haribhai et al., 2011). Moreover, peripherally induced Foxp3⁺ cells consist of a cell subset continuously expressing FOXP3 and a subset of activated CD4⁺ T cells only transiently expressing FOXP3, which did not acquire suppressor function (Hori, 2011; Kuczma et al., 2009a; Miyao et al., 2012). Activation of naive CD4⁺ T cells *in vitro* in the presence of interleukin-2 (IL-2) and transforming growth factor β (TGF- β) generates induced T_{reg} (iT_{reg}) cells able to restore immune homeostasis in *scurfy* mice (Abbas et al., 2013; Chen et al., 2003; Huter et al., 2008; Thornton et al., 2004). Transcriptome analyses of T_{reg} gene signature of activation-induced, iT_{reg}, and activated T_{reg} cells demonstrated that iT_{reg} cells could present a model to study molecular signaling of pT_{reg} cell generation (Hill et al., 2007; Kuczma et al., 2014; Miyao et al., 2012).

Genetic cell-fate mapping suggested that not only heterogeneity but also phenotypic plasticity of the T_{reg} cell lineage, especially in inflammatory environment, results in the presence of



different proportions of CD4⁺ T cells that downregulate FOXP3 expression (Rubtsov et al., 2010; Zhou et al., 2009b). Uncovering how the sustained phenotype of T_{reg} cells is controlled become even more important when it was realized that T_{reg} cells that downregulate FOXP3 expression (exT_{reg} cells) produce inflammatory cytokines, interferon (IFN)- γ and IL-17 (Guo and Zhou, 2015). While downregulation of FOXP3 is required to alleviate the suppressive effect of T_{reg} cells, T_{reg} cell instability exacerbated tissue damage and immune pathology (Belkaid et al., 2002; Sawant and Vignali, 2014). exT_{reg} cells promoted destruction of pancreatic islets and accelerated the onset of diabetes (Zhou et al., 2009b). In rheumatoid arthritis and autoimmune encephalomyelitis (EAE), pathogenic Th17 cells were shown to arise from T_{reg} cells (Bailey-Bucktrout et al., 2013; Komatsu et al., 2014). In contrast, resolution of inflammation may depend on the opposite process of trans-differentiation of Th17 cells into T_{reg} cells (Gagliani et al., 2015). Despite its importance, long-term T_{reg} cell maturation, phenotype stability, and programming of T_{reg} and effector Th cell generation remain little understood (Dominguez-Villar and Hafler, 2018; Shevach, 2018).

Bone morphogenic proteins (BMPs), members of the TGF- β family of cytokines, include activins, growth and differentiation factors, and TGF- β s (Wu and Hill, 2009). They consist of approximately 20 cytokines that control fundamental biological processes including cell migration, apoptosis, adhesion, and differentiation (Bragdon et al., 2011; Carreira et al., 2014). Their activities are highly pleiotropic, often context dependent, and limited to the close vicinity of secreting cells, predisposing them to regulate local tissue homeostasis. In contrast to TGF- β , only a few studies were conducted on immunoregulatory functions of BMPs (Chen and Ten Dijke, 2016; Li and Flavell, 2008). Activin A and BMP2/4 are not able to induce FOXP3 expression in activated CD4⁺ T cells but synergized with the TGF- β to generate iT_{reg} cells (Huber et al., 2009; Lu et al., 2010). *In vitro* studies of signaling inhibitors have shown that BMPs regulate proliferation and activation of CD4⁺ T cells, but the role of BMPs in controlling peripheral T_{reg} cells was not addressed (Martínez et al., 2015; Yoshioka et al., 2012). Recently, we reported that deletion of bone morphogenic protein receptor 1 α (BMPR1 α , Alk-3) in conventional CD4⁺ T cells promotes Th17 cell differentiation, emphasizing the importance of BMPR1 α for Th cell-lineage specification (Browning et al., 2018).

We report that signaling through the BMPR1 α is necessary to control maturation, sustain the phenotype of peripheral T_{reg} cells, and allow for generation of iT_{reg} cells. This last finding suggests that BMPR1 α signaling will also promote upregulation of FOXP3 in CD4⁺ T cells *in vivo* and support generation of pT_{reg} cells. T_{reg} cell-specific deletion of BMPR1 α results in the gradual loss of peripheral T_{reg} cells associated with FOXP3 downregulation, accumulation of mature, senescent T_{reg} cells, and exaggerated responses to stimulation with antigen. During antigenic stimulation, abrogation of BMPR1 α signaling enhances downregulation of FOXP3 in T_{reg} cells and increases proportion of effector Th cells secreting IFN- γ and IL-17 generated from purified T_{reg} cells. This finding underscores the importance of the BMPR1 α in regulating inflammation by controlling T_{reg} cell plasticity and transition between T_{reg} and Th cells. At the molecular level, BMPR1 α deficiency led to upregulation of KDM6B

(JMJD3) demethylase, indicating that chromatin modifications contributing to proinflammatory reprogramming of CD4⁺ effector and T_{reg} cells are regulated by BMPs.

RESULTS

Deletion of the BMPR1 α in T_{reg} Cells Disrupts Homeostasis of the Peripheral T Cell Population

BMPR1 α signaling is required at different stages of thymocyte differentiation, and it is expressed in single positive CD4⁺ conventional and T_{reg} cells in the thymus (Figure S1A; Hager-Theodorides et al., 2014; Jurberg et al., 2015). BMPR1 α is also expressed by Th and T_{reg} cells directly isolated from lymph nodes or peripheral organs or activated *in vitro* and in iT_{reg} cells (Figures S1B, S1C, and S2C; Browning et al., 2018; Kuczman et al., 2014). To examine the role of BMPR1 α in T_{reg} cells, we crossed BMPR1 α conditional knockout mice to transgenic mice expressing creGFP fusion protein controlled by the FOXP3 gene regulatory sequences (Zhou et al., 2008). T_{reg} cells in wild-type mice expressing solely Foxp3^{creGFP} had low levels of GFP reporter, making it difficult to identify T_{reg} cells expressing low and high levels of FOXP3. These two T_{reg} cell subsets have different functions in wild-type mice, with Foxp3^{GFP^{high}} cells having stable suppressor function and the Foxp3^{GFP^{low}} subset demonstrating phenotype plasticity (Komatsu et al., 2009; Kuczman et al., 2009a; Miyao et al., 2012). To ensure that T_{reg} cells expressing low levels of FOXP3 (especially after BMPR1 α is deleted, see below) are readily identified, we introduced another Foxp3^{GFP} reporter, produced in our laboratory, expressing higher levels of GFP to generate Foxp3^{GFP}Foxp3^{creGFP}BMPR1 α ^{-/-} (BMPR1 α ^{TR-/-}) mice (Kuczman et al., 2009b). Co-expression of both transgenic constructs does not affect T cell development, and littermates heterozygous for BMPR1 α expressing only Foxp3^{GFP} or both Foxp3^{GFP} and Foxp3^{creGFP} reporters have the same total numbers and proportions of thymocyte subsets (Figure S1A). This result is consistent with late expression of the cre recombinase, following induction of FOXP3 expression, which does not impair thymocyte recruitment into T_{reg} population. When lymph nodes of 2- to 3-week-old mice were analyzed, the total number of cells and proportions of conventional CD4⁺ and T_{reg} cells were the same between two types of littermates (Figure S1B). However, deletion of one allele of BMPR1 α resulted in increased proportion of T_{reg} cells expressing low levels of FOXP3 (Figure S1B). This demonstrates that even decreased BMP signaling affects T_{reg} cells already in young mice. Complete abrogation of BMPR1 α signaling resulted in moderate reduction in the total proportion of T_{reg} cells but significantly altered proportions of T_{reg} cells expressing high and low levels of FOXP3 residing in lymph nodes and peripheral organs (Figures 1A and S2). Loss of Foxp3^{GFP^{high}} T_{reg} population was associated with low expression of FOXP3 in CD4⁺ T cells (Figure 1B). As BMPR1 α ^{TR-/-} mice aged, we observed loss of T_{reg} cells expressing high levels of FOXP3 (Foxp3^{GFP^{high}}) and increasing proportion of cells expressing low levels of FOXP3 (Foxp3^{GFP^{low}}) indicating disruption of peripheral homeostasis of T_{reg} cells (Figure 1C). In contrast, wild-type mice of various ages continuously had a small population of cells expressing low levels of FOXP3, most likely conventional CD4⁺ T cells that transiently

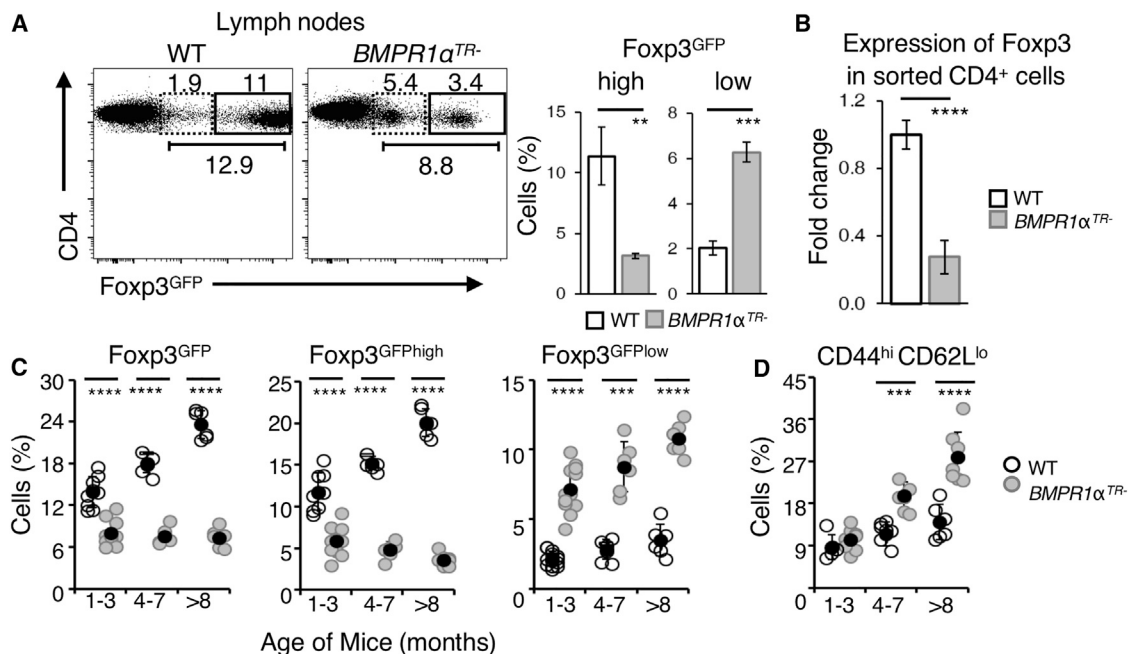


Figure 1. BMPR1 α Signaling Controls Peripheral T_{reg} Cell Homeostasis and Stability

(A) Flow cytometry analysis of Foxp3^{GFP} expression in CD4⁺ T cells isolated from wild-type (WT) and *BMPR1α*^{TR-} 1- to 3-month-old mice. The frequency of Foxp3^{GFP}⁺ cells are means \pm SD pooled from all experiments.

(B) qRT-PCR analysis of FOXP3 mRNA expression in CD4⁺ cells sorted from WT and *BMPR1α*^{TR-} mice. Data are means \pm SD pooled from three independent sorts.

(C) Proportions of total T_{reg} cells (Foxp3^{GFP}) and T_{reg} cells expressing high (Foxp3^{GFP}^{high}) and low (Foxp3^{GFP}^{low}) levels of FOXP3 in the population of lymph node CD4⁺ T cells in 1- to 3-, 4- to 7-, and >8-month-old WT and *BMPR1α*^{TR-} mice.

(D) Proportion of activated (CD44^{hi}CD62L^{lo}) CD4⁺ T cells in the lymph nodes of WT or *BMPR1α*^{TR-} 1- to 3-, 4- to 7-, and >8-month-old mice. For (C) and (D), each dot represents one mouse, the solid black dot represents the average, and vertical lines represent standard deviations. ***p* < 0.01, ****p* < 0.001, *****p* < 0.0001 as determined by Student's *t* test.

See also Figures S1 and S2.

upregulated FOXP3, and an overwhelming majority of T_{reg} cells expressed high levels of FOXP3 (Kuczma et al., 2009a; Miyao et al., 2012). Progressive loss of FOXP3 expression in T_{reg} cells was accompanied by a continuing increase in the subset of activated, conventional CD4⁺ T cells in aging *BMPR1α*^{TR-} mice consistent with compromised T_{reg} cell suppressor function (Figure 1D). In summary, an analysis of CD4⁺ T cell subsets in *BMPR1α*^{TR-} mice underscores an essential role of BMPR1 α in controlling homeostasis and phenotype stability of peripheral T_{reg} cells.

Decreased Phenotype Stability of BMPR1 α -Deficient T_{reg} Cells

To further compare stability of peripheral T_{reg} cells, we adoptively co-transferred equal proportions of T_{reg} cells from wild-type and *BMPR1α*^{TR-} mice expressing high levels of Foxp3^{GFP} into lymphopenic T cell receptor (TCR)- α knockout mice together with naive cells from wild-type mice to provide a source of IL-2 to sustain T_{reg} cell populations (Figure 2A). Transferred wild-type T_{reg} cells retained Foxp3^{GFP} expression and expressed higher levels of CD25, 4-1BB, and KLRG1, markers of effector T_{reg} cells (Figure 2B). In contrast, *BMPR1α*-deficient T_{reg} cells downregulated both Foxp3^{GFP} and CD25 expression; however, CD127 expression was higher than on wild-type T_{reg} cells (Figure 2B).

Transferred *BMPR1α*-deficient T_{reg} cells had low expression of KLRG1 but high expression of CCR6 and IL-23R. CCR6 and IL-23R are receptors regulating homing and promoting differentiation of Th17 cells or their precursors. Higher expression of CCR6 and IL-23R is consistent with increased levels of RORC, IFN- γ , and IL-17 found in donor *BMPR1α*-deficient cells when lymph node cells of recipient mice were stimulated with Con A (Figure 2C). Since donor cells were highly purified T_{reg} cells, this suggested that impaired BMPR1 α signaling increases T_{reg} plasticity and transition between T_{reg} and effector Th cells (Zhou et al., 2009b; Bailey-Bucktrout et al., 2013). Loss of T_{reg} cell phenotype and increased production of inflammatory cytokines were associated with decreased recipient weight when only one T_{reg} cell type, *BMPR1α*-deficient but not *BMPR1α*-sufficient T_{reg} cells, were transferred into lymphopenic mice (Figures 2D–2F). In summary, analysis of T_{reg} cell recipients demonstrates that BMPR1 α is essential to sustain FOXP3 expression and T_{reg} cell suppressor function.

To determine how stable the T_{reg} cell phenotype is in an inflammatory environment, we activated T_{reg} cells sorted from wild-type and *BMPR1α*^{TR-} mice in the presence of bacterial lysate mimicking bacterial infection *in vivo* (Figure 3A). While the majority of T_{reg} cells from normal mice preserved high levels of FOXP3 expression, a large proportion of T_{reg} cells from *BMPR1α*^{TR-}

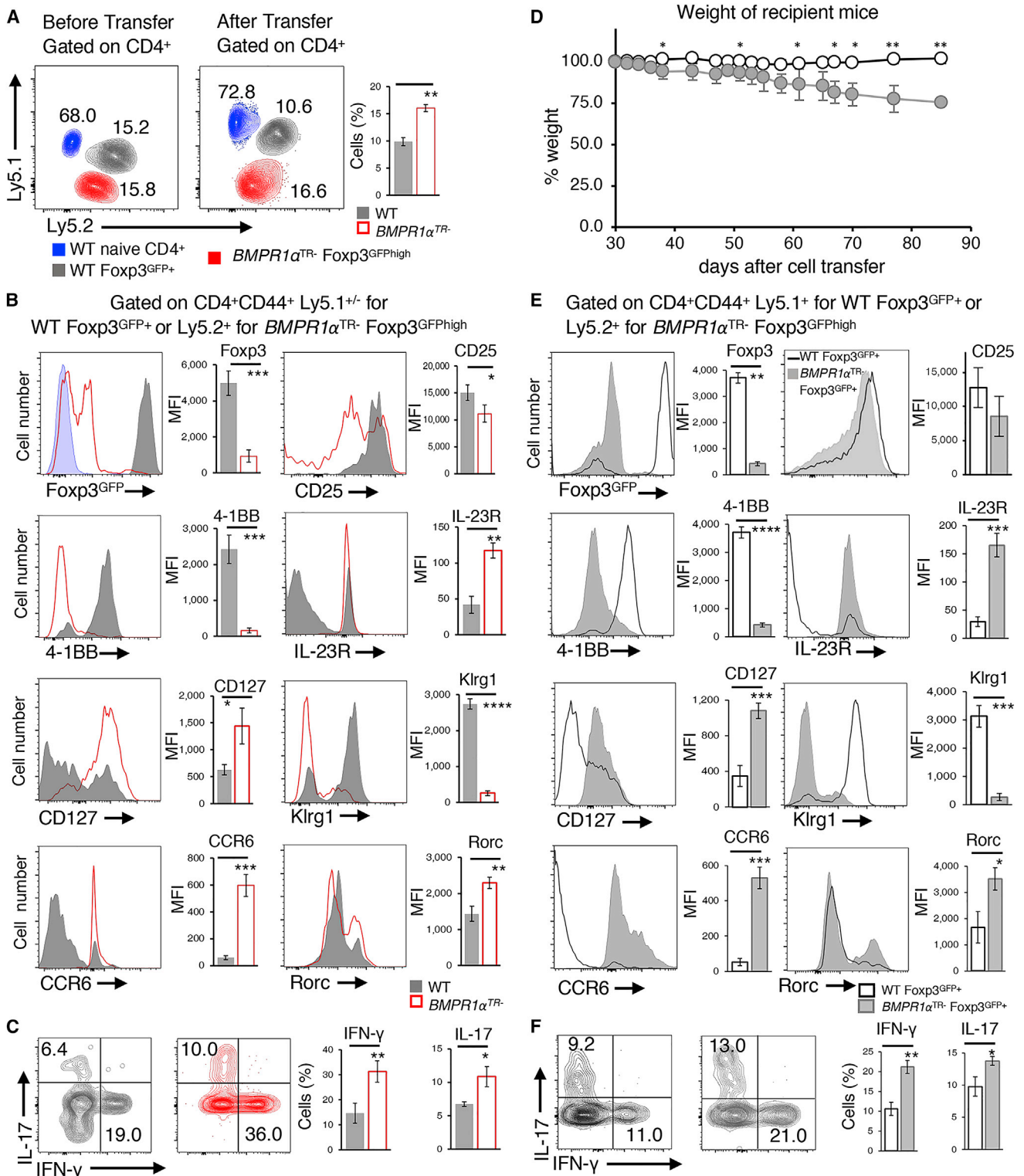


Figure 2. *BMPR1α* Signaling Is Essential to Sustain FOXP3 Expression and T_{reg} Cell Phenotype

(A) Flow cytometry analysis of wild-type (WT Foxp3^{GFP+}Ly5.1⁺Ly5.2⁺) T_{reg} cells, *BMPR1α*-deficient T_{reg} cells expressing high levels of FOXP3 (*BMPR1α*^{TR-}Foxp3^{GFPhigh}Ly5.2⁺) and wild-type naive CD4⁺ T cells (Ly5.1⁺) before (left panel) and after (right panel) co-transfer into TCR α ⁻ recipient mice. Data are representative of four independent analyses. The frequency of T_{reg} cell populations are means \pm SD pooled from all analyses.

(legend continued on next page)

mice downregulated FOXP3. The rate of cell divisions of BMPR1 α -sufficient and -deficient T_{reg} cells was similar, as shown by dilution of cell proliferation dye eFluor670, suggesting that decreasing expression of FOXP3 and not proliferative advantage is responsible for accumulation of exT_{reg} cells. We calculated the probability that a random T_{reg} cell retains FOXP3 expression to be almost two times higher for a wild-type T_{reg} cell (0.85 versus 0.45). Loss of FOXP3 expression was accompanied by increased production of inflammatory cytokines, IFN- γ , and IL-17 (Figure 3B). In conclusion, BMPR1 α signaling is essential to sustain T_{reg} cells in inflammatory conditions and inhibit differentiation of Th effector cells producing IFN- γ and IL-17 (Browning et al., 2018).

Enhanced Antigenic Responses in BMPR1 α ^{TR-} Mice

To test how the lack of BMPR1 α expression affects T_{reg} cell immunoregulatory function, we analyzed antigenic responses in mice immunized with CFA. CD4⁺ T cells from BMPR1 α ^{TR-} mice displayed a more activated phenotype and produced more IFN- γ and IL-17 than wild-type mice (Figures 3C and 3D). BMPR1 α continues to be expressed in effector Th and T_{reg} cells in the draining lymph nodes of immunized mice indicating that BMPR1 α signaling modulates ongoing inflammatory response (Figure 3E). T_{reg} cells in the draining lymph nodes had lower FOXP3 expression in BMPR1 α ^{TR-} than wild-type mice (Figure 3F). However, despite compromised suppressor function, BMPR1 α -deficient T_{reg} cells were able to inhibit proliferation of CD4⁺ T cells in an *in vitro* assay (Figure S3). This is consistent with previous reports that T_{reg} cells present in mouse strains prone to autoimmune diseases had normal suppressor function *in vitro* (Konkel et al., 2017; Shevach, 2018). BMPR1 α -deficient T_{reg} cells expressed lower levels of CD39, 4-1BB, ICOS, and KLRG1 (Figure 3G). CD39 is an ectonuclease directly involved in T_{reg} suppressor function and 4-1BB binding of galectin-9 augments T_{reg} function (Deaglio et al., 2007; Fletcher et al., 2009; Madireddi et al., 2014; So et al., 2008). KLRG1 is upregulated on antigen-activated, highly suppressive T_{reg} cells, so its low expression likely indicates defective terminal differentiation of BMPR1 α -deficient T_{reg} cells (Cheng et al., 2012). Loss of ICOS by T_{reg} cells was associated with instability of FOXP3 expression (Landuyt et al., 2019). BMPR1 α -deficient T_{reg} expressed elevated levels of IL-10 compared to wild-type mice in steady state, but both types of activated T_{reg} cells had similar expression of IL-10 (Figures 3H and 5B).

To further examine how deletion of BMPR1 α impacts immune responses to natural mouse pathogen, we infected wild-type and BMPR1 α ^{TR-} mice with *Citrobacter rodentium* (Crepin et al.,

2016). Infection with *C. rodentium* is widely used to model human infections with enteropathogenic *E. coli* (Collins et al., 2014). We observed a significant loss of T_{reg} cells expressing high levels of FOXP3 associated with increased proportions of proinflammatory cytokine-producing cells in the colon of BMPR1 α ^{TR-} mice demonstrating decreased ability of BMPR1 α -deficient T_{reg} cells to control inflammation *in vivo* (Figure S4). In summary, current data and our earlier report point to the importance of BMPR1 α ligands to target T_{reg} and effector CD4⁺ T cells to constrain inflammation (Browning et al., 2018).

Altered Ontogenesis of BMPR1 α -Deficient T_{reg} Cells

While in 2-month-old wild-type and BMPR1 α ^{TR-} mice conventional CD4⁺ T cells have similar proportions of naive (CD44^{low}CD62L^{high}) and activated (CD44^{high}CD62L^{low}) T cells, expression of maturation markers was different on T_{reg} cells (Figures 4A and 4B). We examined whether loss of BMPR1 α expression is associated with changes in the ontogeny of T_{reg} cell population. Recent evidence supports a model of T_{reg} cell maturation whereby effector T_{reg} cells with an activated phenotype originate from a pool of naive T_{reg} cells expressing high levels of CD62L and lower levels of CD44 (Cheng et al., 2012; Levine et al., 2014; Rosenblum et al., 2011; Toomer et al., 2016). Transition of naive to mature (activated) effector T_{reg} cells is promoted by IL-2, and terminally differentiated T_{reg} cells are sustained by IL-7 (Gratz et al., 2014; Malek et al., 2002; Toomer et al., 2016).

When expression of activation markers was examined on T_{reg} cells in wild-type and BMPR1 α ^{TR-} mice, the overall proportion of T_{reg} cells with activated phenotype was much higher in age-matched BMPR1 α ^{TR-} than in wild-type mice, while the proportion of naive T_{reg} cells was smaller (Figure 4B). In addition, Foxp3^{GFP^{low}} T_{reg} cells predominantly expressed the activated phenotype and Foxp3^{GFP^{high}} T_{reg} cells expressed the naive phenotype (Figure 4C). To compare mature T_{reg} cells in wild-type and BMPR1 α ^{TR-} age-matched mice, we analyzed the expression of CD25, CD39, CD127, and maturation marker KLRG1 (Cheng et al., 2012; Figure 4D). Expression of IL-2 receptor α chain, CD25, was similar on BMPR1 α -deficient and -sufficient T_{reg} cells and did not decrease in aging mice. Thus, altered proportions of naive and mature T_{reg} cells were not caused by decreased sensitivity to IL-2 (Yu et al., 2009). Mature T_{reg} cells in BMPR1 α ^{TR-} mice express higher levels of CD127, a receptor for IL-7, which maintains memory T_{reg} cells in peripheral tissues (Gratz et al., 2013). However, they express low levels of KLRG1 and CD39, demonstrating that terminal maturation and the immunosuppressive function of these cells are impaired, and

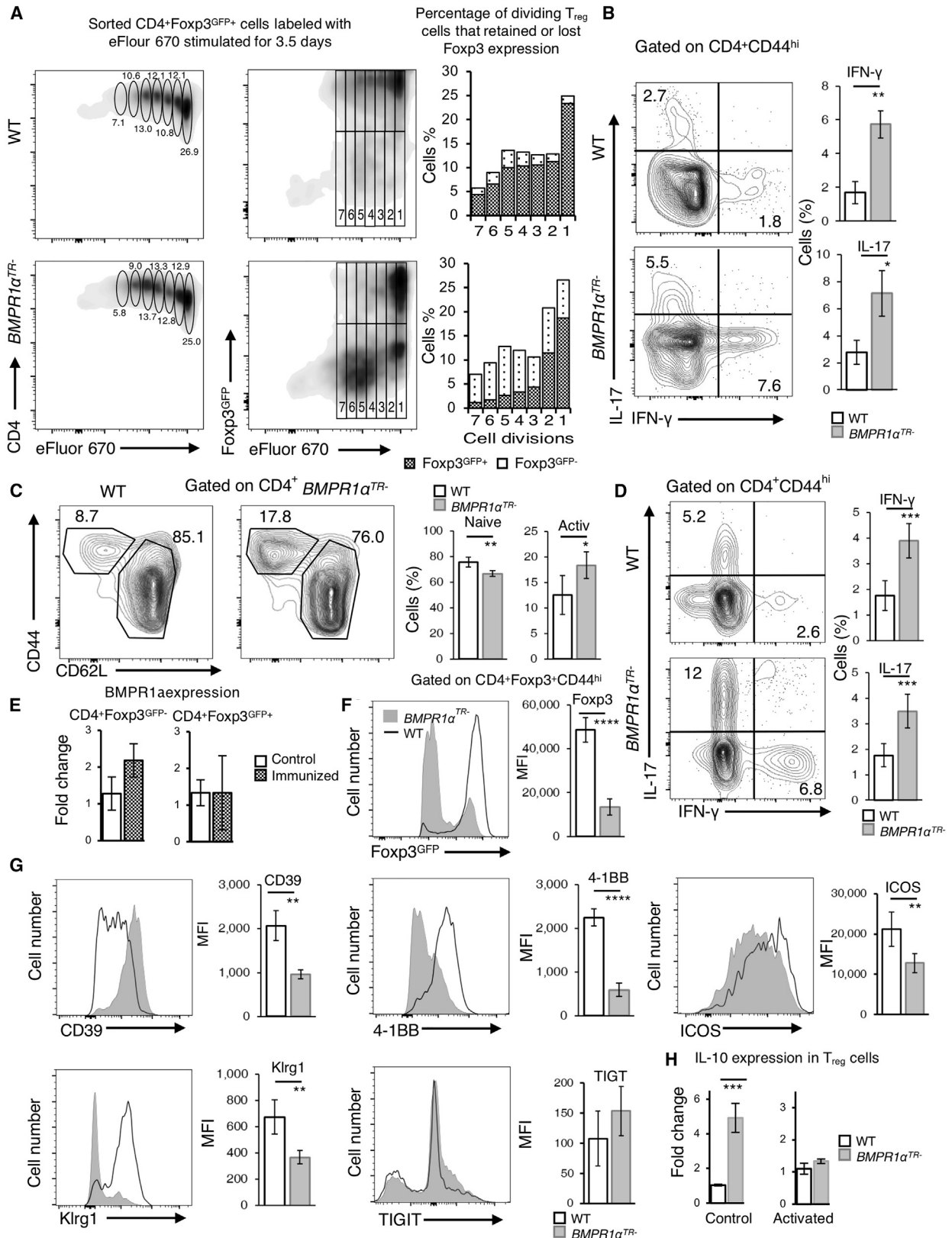
(B) Flow cytometry analysis of the indicated molecules expressed by donor WT and BMPR1 α ^{TR-} T_{reg} cells. Histograms are representative of four independent analyses. Expression of respective molecules by wild-type (filled gray histograms) or BMPR1 α -deficient (open red histograms) donor T_{reg} cells and summary of expression data showing mean fluorescence intensity (MFI) of at least three mice analyzed (bar graphs).

(C) Flow cytometry analysis of cytokine production by transferred WT (left panel) and BMPR1 α ^{TR-} (right panel) T_{reg} cells restimulated *in vitro*. Contour plots are representative of four independent analyses. The frequency of cytokine-producing cells are means \pm SD pooled from all experiments.

(D) Weight of TCR α ⁻ mice receiving transfer of WT naive CD4⁺ T cells and WT (open black circles) or BMPR1 α -deficient (filled gray circles) T_{reg} cells. Data are representative of three mice per group.

(E) Flow cytometry analysis of molecules expressed by donor WT (open black histograms) and BMPR1 α -deficient (filled gray histograms) T_{reg} cells isolated from TCR α ⁻ recipient mice and summary of expression data showing MFI of three mice analyzed (bar graphs).

(F) Production of IL-17 and IFN- γ by transferred WT (left panel) or BMPR1 α ^{TR-} (right panel) T_{reg} cells restimulated *in vitro*. Plots show representative data of three mice analyzed. MFI data are means \pm SD from all experiments. *p < 0.05, **p < 0.01, ***p < 0.001, ****p < 0.0001 as determined by Student's t test.



(legend on next page)

they may not generate robust effector T_{reg} cells (Cheng et al., 2012).

To determine the cause of altered proportions of $Foxp3^{GFP^{high}}$ and $Foxp3^{GFP^{low}}$ T_{reg} cells in $BMPR1\alpha^{TR-}$ mice, we examined fractions of proliferating cells in these populations. Bromodeoxyuridine (BrdU) incorporation revealed significant difference in a steady-state proliferation between T_{reg} cells in wild-type and $BMPR1\alpha^{TR-}$ mice (Figure 5A). While $Foxp3^{GFP^{high}}$ cells were more proliferatively active in wild-type mice, $Foxp3^{GFP^{low}}$ T_{reg} cells divided more than $Foxp3^{GFP^{high}}$ in $BMPR1\alpha^{TR-}$ mice. In addition, a much lower fraction of all T_{reg} cells incorporated BrdU in $BMPR1\alpha^{TR-}$ mice. We propose that decreased proliferation is likely not enough to sustain the size of the $Foxp3^{GFP^{high}}$ T_{reg} subset and results in a low proportion of naive T_{reg} cells as $BMPR1\alpha^{TR-}$ mice age. Thus, phenotypic and BrdU incorporation analyses show that T_{reg} cell maturation in $BMPR1\alpha^{TR-}$ mice is associated with a low proliferative capacity of $Foxp3^{GFP^{high}}$ T_{reg} cells, progressive loss of FOXP3 expression, and accumulation of $Foxp3^{GFP^{low}}$ T_{reg} cells with mature phenotype. Decreased cell proliferation also reduced the expansion of $BMPR1\alpha$ -deficient iT_{reg} cells *in vitro* (Kuczma et al., 2014).

Signaling Modules Controlled by $BMPR1\alpha$

To determine how $BMPR1\alpha$ signaling affects molecular circuits controlling T_{reg} cell lineage, we examined genes expressed in $BMPR1\alpha$ -deficient $Foxp3^{GFP^{high}}$ and $Foxp3^{GFP^{low}}$ and wild-type $Foxp3^{GFP^{+}}$ T_{reg} cells using the NanoString inflammation panel (Figure 5B). This analysis identified 196 and 230 genes differentially expressed between $Foxp3^{GFP^{high}}$ or $Foxp3^{GFP^{low}}$ and wild-type $Foxp3^{GFP^{+}}$ T_{reg} cells (145 genes differentially expressed between $Foxp3^{GFP^{high}}$ and $Foxp3^{GFP^{low}}$ and wild-type $Foxp3^{GFP^{+}}$ T_{reg} cells) (Table S1).

Gene set enrichment analysis defined cytokine activity, secretion, receptor binding, and signal transduction as major molecular functions and immune and inflammatory responses as biological processes regulated by differentially expressed genes. Transcript levels of proinflammatory cytokines and transcription factors, including IFN- γ , IL-17, IL-6, RORC, and IRF4 were higher in $BMPR1\alpha$ -deficient T_{reg} cells (Figure 5B). Expression of RORC in T_{reg} cells is considered evidence of phenotypic plasticity and functional adaptation that underlies transition into Th17 cells (Ivanov et al., 2006; Komatsu et al., 2014). This im-

plies a less stable phenotype of $BMPR1\alpha$ -deficient T_{reg} cells, more so resembling T_{reg} cells co-expressing Th-lineage-specific transcription factors with a decreased ability to control inflammation and susceptible to lineage dedifferentiation (Blatner et al., 2012; Saito et al., 2016; Zhou et al., 2009b). This interpretation is consistent with observed downregulation of FOXP3 and enhanced production of Th1/Th17 cells in inflammatory conditions (Gao et al., 2015; Komatsu et al., 2014; Yang et al., 2008a).

A set of differentially expressed genes included CDKN1A ($p21^{Cip1}$), a cell-cycle inhibitor associated with cell maturation and senescence, which was expressed at much higher levels in T_{reg} cells in $BMPR1\alpha^{TR-}$ mice (Figure 5B; Muñoz-Espín et al., 2013). CDKN1A controls $CD4^{+}$ T cell responses to antigen and generation of memory or anergic cells (Arias et al., 2007). We postulate that in $BMPR1\alpha$ -deficient T_{reg} cells overexpression of CDKN1A inhibits proliferation and renewal of immature T_{reg} subset while promoting maturation and senescence.

Current analyses of T_{reg} cell stability and our previous report demonstrated that $BMPR1\alpha$ regulates signaling circuits promoting generation of proinflammatory cells affecting both T_{reg} and conventional $CD4^{+}$ T cells (Browning et al., 2018). We have also previously shown that upregulation of $Foxp3$ and generation of iT_{reg} cells is impaired by $BMPR1\alpha$ deficiency (Figure S1C; Kuczma et al., 2014). Thus, gene-expression analysis of sorted T_{reg} cells was accompanied by RNA sequencing (RNA-seq) analysis of iT_{reg} cells, generated from $BMPR1\alpha$ -sufficient and -deficient $CD4^{+}$ cells, which found 804 genes differentially expressed (Figure 6A; Table S2). Principal-component analysis (PCA) demonstrated substantially different transcriptome landscape of $BMPR1\alpha$ -deficient and -sufficient iT_{reg} cells (Figure 6B). $BMPR1\alpha$ -deficient iT_{reg} cells expressed elevated levels of transcripts associated with proinflammatory Th cell lineages, including Th17 cells, like RORC, RORA, MAF, IKZF4 (EOS), CCR6, and signaling molecules like SOCS13 and CISH (Figure 6C; Ciofani et al., 2012; Yosef et al., 2013). At the same time, genes associated with iT_{reg} cell-lineage specification like FOXP3, HOPX, PDE3B, and CREM were downregulated (Figures 6C and S1C). Gene ontology analysis defined cytokine activity, receptor binding, and signaling as top molecular functions of differentially expressed iT_{reg} genes.

Figure 3. Deletion of the $BMPR1\alpha$ Gene Regulates T_{reg} Cell Stability and Enhances Antigenic Responses of Effector $CD4^{+}$ T Cells in Immunized Mice

(A) Flow cytometry analysis of cell division and $Foxp3^{GFP}$ expression by T_{reg} cells sorted from WT and $BMPR1\alpha^{TR-}$ mice and activated in the presence of bacterial lysate for 3.5 days. Left panels show the percentage of dividing cells and right panels and graphs show the percentage of T_{reg} cells after each cell division that retained (dark pattern) or lost (dotted pattern) $Foxp3^{GFP}$ expression. Representative data of one of three experiments are shown.

(B) Flow cytometry analysis of cytokine production by the T_{reg} cells activated in the presence of bacterial lysate.

(C) Flow cytometry analysis of proportions of naive ($CD44^{lo}CD62L^{hi}$) and activated ($CD44^{hi}CD62L^{lo}$) $CD4^{+}$ T cells in WT and $BMPR1\alpha^{TR-}$ mice injected with CFA in the footpad and analyzed after 2 weeks.

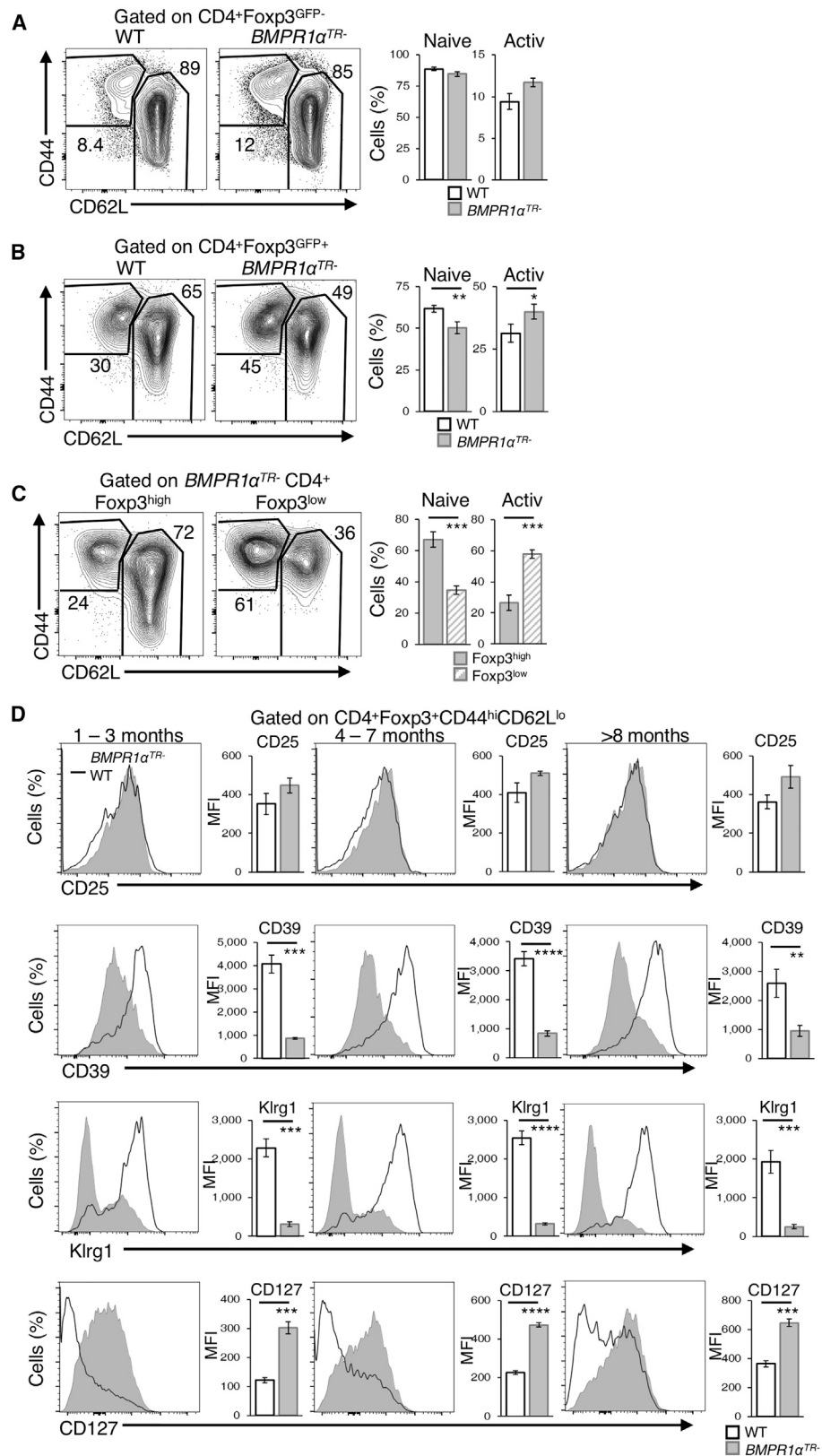
(D) Flow cytometry analysis of cytokine production by effector $CD4^{+}$ T cells.

(E) qRT-PCR analysis of $BMPR1\alpha$ transcript levels in Th ($CD4^{+}Foxp3^{GFP^{-}}$) and T_{reg} ($CD4^{+}Foxp3^{GFP^{+}}$) cells sorted from draining lymph nodes of control and immunized WT mice.

(F and G) Expression of $Foxp3^{GFP}$ (F) and indicated surface markers (G) in T_{reg} cells in the draining lymph nodes of WT and $BMPR1\alpha^{TR-}$ mice immunized with CFA.

(H) qRT-PCR analysis of IL-10 transcript levels in T_{reg} cells sorted directly from WT and $BMPR1\alpha^{TR-}$ mice (left plot) or activated *in vitro* (right plot). Histograms, contour plots, and qRT-PCR are representative of three independent analyses. The frequency of naive, activated, IFN- γ^{+} and IL-17 $^{+}$ cells, and surface marker MFI are means \pm SD from all experiments. * $p < 0.05$, ** $p < 0.01$, *** $p < 0.001$, **** $p < 0.0001$ as determined by Student's t test.

See also Figure S4.



(legend on next page)

Network Analysis of Gene Expression

Differential gene-expression analysis established that the same set of effector Th cell-associated genes is overexpressed in *BMPR1 α* -deficient $CD4^+$ cells stimulated to become iT_{reg} cells and in activated, effector $CD4^+$ cells (Browning et al., 2018). To understand mechanistically how the same set of genes promotes Th17 cell bias and prevents iT_{reg} cell generation, we used a system approach and generated weighted gene co-expression networks (WGCNA) (Chou et al., 2014; Langfelder and Horvath, 2008; Zhang and Horvath, 2005). This approach looks at correlations of gene-expression levels and connects genes with the same pattern of expression profiles. Comparison of network topology identifies genes (nodes) and their interactions (edges) specific for, or different between, cell populations and provides insight into how similar signaling circuits (network modules) in analyzed cell populations are. We reasoned that functional changes observed in *BMPR1 α* -deficient and -sufficient iT_{reg} cells are directed by differential expression of transcription factors. Thus, using the WGCNA approach, we have generated networks such that at least one node of each edge is a transcription factor or a DNA modifying enzyme differentially expressed (fold change ≥ 1.5 and statistically significant difference) between activated wild-type and *BMPR1 α* -deficient $CD4^+$ T cells (611 genes) or wild-type and *BMPR1 α* -deficient iT_{reg} cells (805 genes, 217 genes were common between activated and iT_{reg} cells). Networks generated for activated wild-type and *BMPR1 α* -deficient $CD4^+$ T cells included 1,408 and 1,844 edges, respectively, and networks generated for wild-type and *BMPR1 α* -deficient iT_{reg} cells contained 1,307 and 2,757 edges (Table S3A–D).

To further examine how similar are network topologies, we looked at what interactions are common or different between examined cell subsets (Figure 6D). We found that the proportion of edges shared by *BMPR1 α* -deficient and -sufficient iT_{reg} cells (10.1%) is similar to the proportion of edges shared between *BMPR1 α* -deficient iT_{reg} cells and activated *BMPR1 α* -deficient or -sufficient effector $CD4^+$ cells (10.1 and 9.7%, respectively). In contrast, lower proportions of network edges are shared by wild-type iT_{reg} cells and *BMPR1 α* -deficient and -sufficient effector $CD4^+$ cells (5.0 and 7.0%, respectively). Thus, comparison of network topologies suggests higher similarities of *BMPR1 α* -deficient iT_{reg} cells to effector $CD4^+$ T cells than to iT_{reg} cells generated from wild-type $CD4^+$ T cells.

To examine how transcription factors associated with T cell activation or generation of iT_{reg} cells define phenotype of respective cells, we analyzed transcription factors constituting network nodes in each cell subset (Figure 6D). We found that of 25 transcription factors engaged in four networks only three (MYCN, SOX13, and TFAP2A) are specific for an individual subset, and the rest are expressed in more than one subset. This contrasts

with network edges, where almost all interactions are specific for individual subsets (Figure 6D). This result indicates that Th specification is defined mainly by differences in interactions between transcription factors and network molecules with only minor contribution of transcription factors specific for individual Th subsets. Thus, our analysis corroborates earlier observations that the limited number of transcriptional regulators confer a diverse array of individual and context-dependent functions and that Th specification is determined by combinatorial involvement of a limited number of core transcription factors (Fu et al., 2012; Hill et al., 2007; Shih et al., 2014; Yosef et al., 2013). This interpretation is further illustrated by analysis of RORC subnet, which contributes to networks of activated *BMPR1 α* -deficient and -sufficient Th cells and *BMPR1 α* -deficient but not wild-type iT_{reg} cells (Figures 6D and 6E). Genes regulated by RORC in *BMPR1 α* -deficient iT_{reg} cells include transcription factors FOXP3, IKZF4 (EOS), EOMES, cytokines IL-6, IL-17, signaling molecules SHIP, NOD1, and activation molecules 4-1BB (TNFRSF9), RANKL (TNFSF11) known to regulate both T_{reg} and Th cell generation and stability (Curran et al., 2013; Kara et al., 2015; Morikawa and Sakaguchi, 2014; Sharma et al., 2013). Network analysis suggests that impaired generation of *BMPR1 α* -deficient iT_{reg} cells is explained by the presence of regulatory circuits characteristic for activated effector Th cells and suggests that *BMPR1 α* signaling is important to silence transcriptional modules shared with these cells.

Epigenetic Changes Are Associated with *BMPR1 α* Deficiency in T_{reg} and iT_{reg} Cells

Network analyses showed a broad impact of *BMPR1 α* signaling on transcriptional regulation of $CD4^+$ T cells, affecting gene expression controlling various cell functions. To identify a common mechanism that may explain a significant range of observed phenotypic changes in examined cells, we analyzed a set of genes differentially expressed in both *BMPR1 α* -sufficient and -deficient T_{reg} and iT_{reg} cell types. KDM6B demethylase, an antagonist of polycomb repressive complex 2 (PRC2), which sustains repressive trimethylation of H3K27, was found to be expressed higher in activated but lower in iT_{reg} cells generated from wild-type $CD4^+$ T cells compared to *BMPR1 α* -deficient cells (Figure 7A). In wild-type $CD4^+$ T cells, iT_{reg} cell generation is accompanied by downregulation of KDM6B, while in *BMPR1 α* -deficient cells expression of KDM6B remains high. High expression of KDM6B was also found in T_{reg} cells directly isolated from *BMPR1 α* ^{TR-} mice (Figure 7B). CDKN1A, a target of KDM6B, was found upregulated in *BMPR1 α* -deficient cells in NanoString and RNA-seq analyses (Figures 5B and 6C). In $CD4^+$ T cells, KDM6B promotes proinflammatory immune responses and enhances cellular senescence consistent with the observed elevated proportion of mature T_{reg} cells and increased antigenic response

Figure 4. *BMPR1 α* Controls Maturation of Peripheral T_{reg} Cells

(A and B) Flow cytometry analysis of naive ($CD44^loCD62L^hi$) and activated ($CD44^hiCD62L^lo$) conventional $Foxp3^-CD4^+$ (A) and in T_{reg} (B) cells. (C) Expression of maturation markers on $Foxp3^{GFP^{high}}$ and $Foxp3^{GFP^{low}}$ T_{reg} cells from 2-month-old *BMPR1 α* ^{TR-} mice. Data are representative of three mice per genotype. The frequency of cells are means \pm SD pooled from all experiments. (D) Flow cytometry histograms of indicated surface markers on activated $CD4^+$ T_{reg} cells from 1- to 3-, 4- to 7-, and >8-month-old WT and *BMPR1 α* ^{TR-} mice. At least three mice per genotype per age group were analyzed. MFI data are means \pm SD from all experiments. * $p < 0.05$, ** $p < 0.01$, *** $p < 0.001$, **** $p < 0.0001$ as determined by Student's t test.

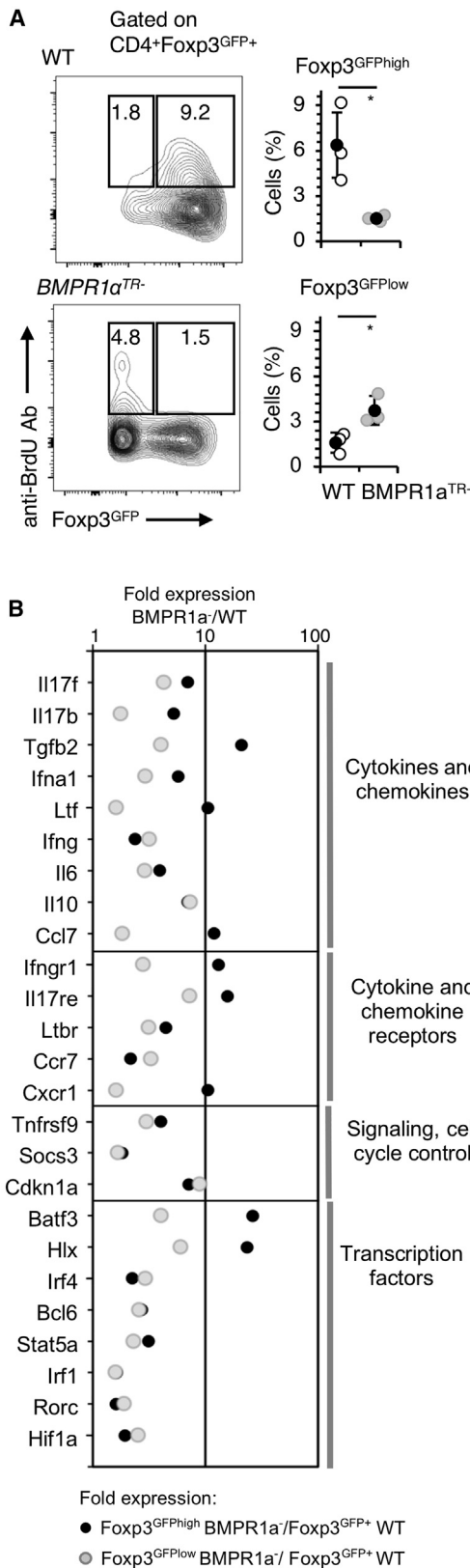


Figure 5. BMPR1 α Controls Proliferation of T_{reg} Cells, and BMPR1 α -Deficient T_{reg} Cells Co-express Effector Th-Lineage Genes

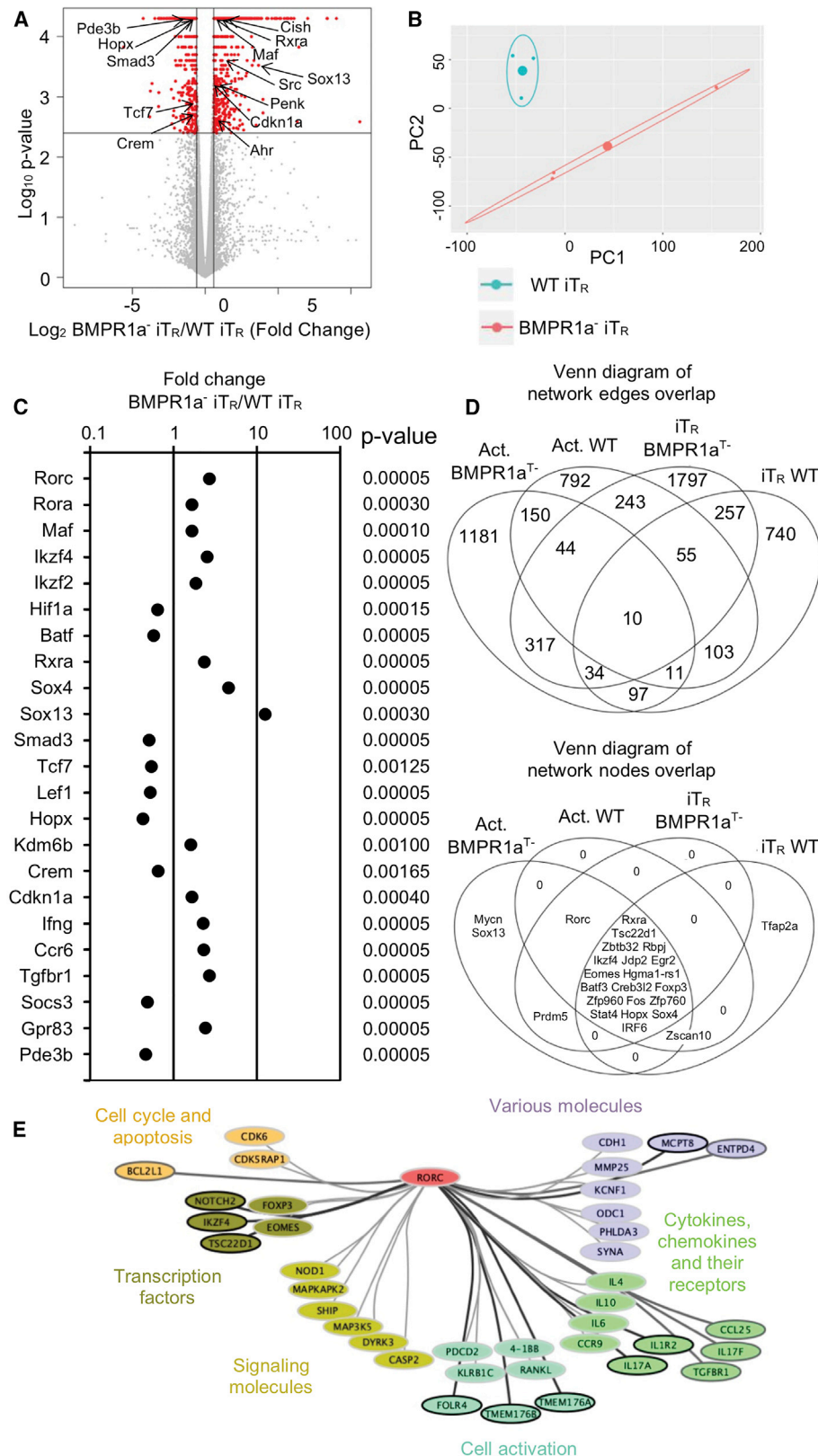
(A) Flow cytometry analysis of BrdU incorporation by T_{reg} cells from 3-month-old WT and BMPR1 α ^{TR-} mice. Plots show the percentage of T_{reg} cells from WT (open black circles) or BMPR1 α ^{TR-} (closed gray circles) mice incorporating BrdU and expressing high and low levels of FOXP3. Each dot represents one mouse. Solid black dots represent the average, and vertical lines represent standard deviations. *p < 0.05 as determined by Student's t test.

(B) NanoString analysis of the fold-change expression of genes differentially expressed in BMPR1 α -deficient Foxp3^{GFP^{high}} or Foxp3^{GFP^{low}} and WT Foxp3^{GFP+} T_{reg} cells, related to inflammatory cytokines and chemokines, signaling and cell-cycle control, and transcription factors.

in BMPR1 α ^{T-} mice (Salminen et al., 2014). Previous reports showed that KDM6B-controlled upregulation of CDKN1A and CDKN2A (p16^{Ink4}) not only regulated the cell cycle but also inhibited reprogramming into self-renewing pluripotent stem cells (Zhao et al., 2013). This KDM6B activity promotes cell maturation and opposes BMPs, which, through BMPR1 α signaling, maintains cell stemness (Li et al., 2012; Ying et al., 2003). Consistent with these reports, CDKN1A expression in T cells was found to depend on the epigenetic status of DNA and was upregulated by histone deacetylase inhibitors (Selma Dagtas and Gilbert, 2010).

To examine how KDM6B impacts T_{reg} cells, sorted T_{reg} cells from wild-type and BMPR1 α ^{TR-} mice were stimulated *in vitro* in the presence of IL-2 and KDM6B inhibitor, GSK-J4 (Ntziachristos et al., 2014). We found that, in the presence of the inhibitor, FOXP3 expression was increased (Figure 7C). Inhibition of KDM6B in naive BMPR1 α -deficient and wild-type CD4⁺ T cells stimulated *in vitro* with IL-2 and TGF- β in the presence of the KDM6B inhibitor also upregulated FOXP3 expression (Figure 7D). An opposite effect of KDM6B inhibition was observed for Th17 cells, where KDM6B inhibition resulted in lower proportion of Th17 cells, as evidenced by decreased expression of RORC and IL-17 (Figure 7E). In summary, inhibition of KDM6B promotes generation of iT_{reg} cells and inhibits generation of Th17 cells.

Thus, our data suggest that, as previously found for other cell types, upregulation of KDM6B induces epigenetic changes modulating expression of a number of genes, including CDKN1A. To further investigate the mechanism of BMPR1 α signaling, we analyzed epigenetic modifications of chromatin associated with the CDKN1A gene. Chromatin immunoprecipitation demonstrated a decreased association of H3K27me3 with CDKN1A gene in BMPR1 α -deficient T_{reg} cells (Figure 7F). Chromatin analysis also showed similar levels of repressive H3K27me3 modifications in FOXP3 gene but decreased levels in RORC gene. Loss of repressive epigenetic marks correlates with elevated transcript levels for CDKN1A and RORC in BMPR1 α -deficient T_{reg} cells (Figure 5B). Co-expression of RORC and FOXP3 was reported to regulate the T_{reg}/Th17 cell phenotype and was detected in subsets of T_{reg} cells in inflammatory conditions and in tumors (Blatner et al., 2012; Ren and Li, 2017; Yang et al., 2016). In summary, chromatin analysis links epigenetic changes with overexpression of CDKN1A and RORC and provides a mechanistic cue for decreased proliferation and stability of BMPR1 α -deficient T_{reg} cells.



(legend on next page)

DISCUSSION

We report that abrogation of BMPR1 α signaling in T_{reg} cells leads to unstable expression and gradual loss of FOXP3. Mature T_{reg} cells expressing low levels of FOXP3 dominate aging BMPR1 α ^{TR-} mice, while the naive T_{reg} subset, still expressing high levels of FOXP3, is severely reduced. While upregulation of activation markers in response to antigenic stimulation is necessary for suppressor function of T_{reg} cells, loss of BMPR1 α signaling is associated with accelerated aging and decreased renewal of BMPR1 α -deficient T_{reg} cells (Levine et al., 2014; Toomer et al., 2016). This is shown by their altered phenotype, lower proportion of proliferating cells, and upregulation of the cell-cycle inhibitor and senescence marker CDKN1A. The reduced suppressor function of T_{reg} cells in aging BMPR1 α ^{TR-} mice is demonstrated by the accumulation of an increased proportion of activated effector CD4⁺ Th cells *in situ*. Phenotypic and functional changes of T_{reg} cells in BMPR1 α ^{TR-} mice are accelerated and amplified in inflammatory or lymphopenic conditions. In immunized mice, an elevated proportion of CD4⁺ Th cells responds to immunization and produces IFN- γ and IL-17, while T_{reg} cells expressed low levels of surface molecules known to promote their suppressor function. These changes were observed even in young BMPR1 α ^{TR-} mice, which still have a significant population of T_{reg} cells expressing high levels of FOXP3. We postulate that in the absence of BMPR1 α signaling T_{reg} cells lose their fitness as demonstrated by the loss of FOXP3, acquisition of maturation markers, lower proliferation, and renewal. Increased expression of maturation markers in a steady state is an evidence of accelerated senescence and is consistent with the known role of BMPs to regulate progenitor cell renewal and differentiation of embryonic and tissue-specific stem cells including T cell progenitors (Li et al., 2012; Varas et al., 2003; Ying et al., 2003).

Uncovering the role of BMPR1 α in T_{reg} cells complements our earlier reports on the role of this receptor in T cell ontogeny and in regulating Th cell differentiation. Deleting BMPR1 α in CD4⁺ T cells impairs generation of iT_{reg} cells and promotes pro-inflammatory function of TGF- β by supporting differentiation of Th17 cells (Browning et al., 2018; Kuczma et al., 2014). These data are consistent with reports demonstrating that inhibition of the BMP signaling in rheumatoid arthritis patients augmented inflammation induced by IL-17 and that BMPs ameliorated intestinal and renal inflammation (Maric et al., 2012; Takabayashi et al., 2014; Varas et al., 2015; Zeisberg et al., 2003). Our report reveals that BMPR1 α is not only an important regulator of embryonic development and stem/progenitor cell-fate decisions but

also controls immune homeostasis and inflammation (Bragdon et al., 2011; Miyazono et al., 2010).

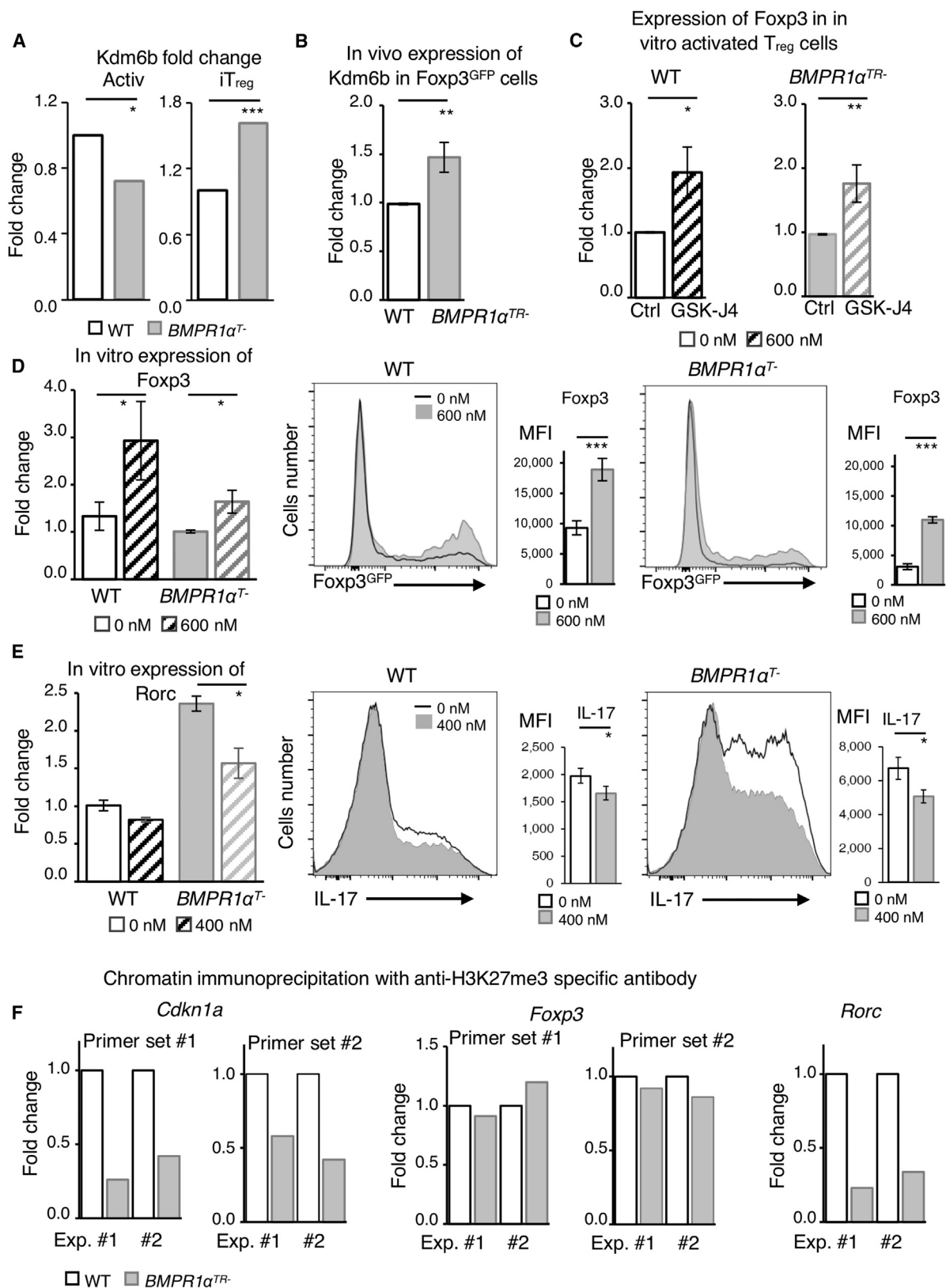
To gain mechanistic insight on the role of BMPR1 α in regulatory cells, we analyzed gene-expression profiles and demonstrated higher expression of canonical transcription factors, cytokines, and cytokine receptors associated with effector Th1/Th17 lineages in T_{reg} and iT_{reg} cells deficient in BMPR1 α . Expression of lineage specification transcription factors was reported in T_{reg} cells still expressing FOXP3 but progressing to acquire Th cell effector phenotype consistent with our results (Beriou et al., 2009; Radhakrishnan et al., 2008; Ren and Li, 2017; Voo et al., 2009; Zhou et al., 2009a). Genes overexpressed in BMPR1 α -deficient T_{reg} cells included transcription factors RORC, BATF3, IRF4, BCL6, and STAT5A, cytokines and cytokine receptors IL-17 and IL-17R, LTF, and IL-10, known to regulate balance between T_{reg} and Th1/Th17 cell lineages, identifying role of BMPR1 α in maintaining T_{reg} cells in peripheral tissues.

While PCA confirmed differences between BMPR1 α -sufficient and -deficient iT_{reg} cells, network analysis explained how a limited set of transcription factors, differentially expressed by activated and iT_{reg} cells, generated phenotypic plasticity. This analysis identified RORC as a signaling hub controlling molecular circuits in the respective populations. In particular, RORC expression correlated with expression of FOXP3, EOMES, IKZF4, NOTCH2, and TSC22D1, transcription factors known to regulate T_{reg} and Th17 cells (Lupar et al., 2015; Qin et al., 2017; Rong et al., 2016; Sharma et al., 2013; Yang et al., 2008b). Signaling modules controlled by RORC are absent in wild-type iT_{reg} cells, which points to the importance of BMPR1 α signaling in iT_{reg} cell generation.

To determine how molecular features of Th cells are established in BMPR1 α -deficient cells, we examined differentially expressed genes and found KDM6B and CDKN1A overexpressed in both BMPR1 α -deficient T_{reg} and iT_{reg} cells. CDKN1A controls the proliferation of activated T cells and sustains T cell anergy following treatment with histone deacetylase inhibitors (Arias et al., 2007; Selma Dagtas and Gilbert, 2010). Deacetylase inhibitors have the same effect as increased activity of KDM6B to promote gene transcription, and KDM6B was reported to alter cell senescence by upregulating CDKN1A (Zhao et al., 2013). Abrogation of the BMPR1 α signaling in T_{reg} cells leads to upregulation of CDKN1A, especially decreasing proliferation and renewal of T_{reg} cells expressing high levels of FOXP3, which need to be activated to contain T cell activation of effector T cells (Levine et al., 2014; Vahl et al., 2014). This explains increased accumulation of activated effector CD4⁺ T cells in BMPR1 α ^{TR-} mice *in situ* and in response to immunization. This interpretation is consistent with a

Figure 6. Abrogation of BMPR1 α Signaling Alters Gene Expression in iT_{reg} Cells

- (A) Volcano plot of genes differentially expressed in RNA-seq analysis of iT_{reg} cells from BMPR1 α -sufficient and -deficient CD4⁺ T cells.
 (B) Principal-component analysis of genes expressed by BMPR1 α -sufficient and -deficient iT_{reg} cells. Small dots indicate component values for individual samples, and large dots indicate average value for three samples.
 (C) Fold-change expression and p values of genes controlling Th-lineage specification and T_{reg} suppressor functions and differentially expressed in RNA-seq analysis of iT_{reg} cells from WT and BMPR1 α ^{TR-} mice.
 (D) Venn diagrams of genes (nodes, top diagram) and interactions (edges, bottom diagram) comparing topologies of gene co-expression networks generated for WT and BMPR1 α -deficient, activated effector CD4⁺ Th and iT_{reg} cells. All edges were present in networks with p > 0.66. Numbers of edges and nodes are shown on diagrams.
 (E) Co-expression subnet of RORC transcription factor. Network shows genes co-expressed with RORC in BMPR1 α -deficient iT_{reg} cells (light gray thin edge and ellipse border line), wild-type (black thick edge and ellipse border line), and BMPR1 α -deficient (dark gray thick edge and ellipse border line) activated CD4⁺ cells.



(legend on next page)

recent report that epigenetic changes promoting CDKN1A upregulation in intestinal T_{reg} cells led to a loss of immune homeostasis and onset of spontaneous colitis (Obata et al., 2014). Thus, as previously reported, T_{reg} cell senescence may be a factor in the progression of chronic autoimmune diseases (Fessler et al., 2017).

KDM6B is expressed at low levels in naive CD4⁺ T cells and is upregulated upon T cell activation, reducing the repressive H3K27 trimethylation mark specifically in the genetic loci of *RORC*, *IL-17*, and *IL-22* genes, promoting Th17-lineage specification (Liu et al., 2015). Consistent with previous report, overexpression of KDM6B in BMPR1 α -deficient CD4⁺ T cells is associated with enhanced Th17 and impaired iT_{reg} cell differentiation and reduced stability of peripheral T_{reg} cells (Browning et al., 2018). Inhibition of KDM6B in T_{reg} and iT_{reg} cells increased FOXP3 expression and generation of iT_{reg} cells while decreasing RORC expression and production of IL-17. This result provides a link between KDM6B overexpression, BMPR1 α signaling, and Th/T_{reg} cell-lineage specification.

To further assess epigenetic modifications in BMPR1 α -deficient T_{reg} cells, we examined chromatin methylation associated with gene loci encoding CDKN1A, RORC, and FOXP3. Chromatin immunoprecipitation shows lower methylation of histone H3 at lysine 27 in BMPR1 α -deficient than in wild-type T_{reg} cells at CDKN1A and RORC loci. There was no difference in the extent of H3K27me3-repressive marks for the FOXP3 gene. This result suggests that lower and unstable expression of FOXP3 in BMPR1 α -deficient T_{reg} cells may not be directly dependent on epigenetic modifications at the *FOXP3* gene locus but rather result from permissive chromatin modifications and upregulation at genes encoding transcription factors like RORC, which promote effector Th cell generation. Our results are consistent with reports demonstrating that inhibition of enhancer of zeste homolog 2, a histone H3K27 methyltransferase of the PRC2, compromised T_{reg} cell function in tumors and autoimmune diseases (Wang et al., 2018; Xiao et al., 2020). Together, published reports and our data suggest that BMPR1 α and its ligands modulate T_{reg} cells by controlling KDM6B and modifying repressive chromatin marks imposed by PRC2.

In summary, we have established that BMPR1 α controls molecular circuits differentially present in effector and T_{reg} cells underscoring the role of this receptor in lineage specification. We have identified the epigenetic modifier KDM6B and cell-cycle and senescence regulator CDKN1A as molecules that, in

response to BMPR1 α , modulate T_{reg} cell fitness and transition between T_{reg} and Th1/Th17 cells. This indicates that BMPs not only sustain tissue homeostasis but control essential mechanisms of adaptive immune response.

STAR★METHODS

Detailed methods are provided in the online version of this paper and include the following:

- KEY RESOURCES TABLE
- RESOURCE AVAILABILITY
 - Lead Contact
 - Materials Availability
 - Data and Code Availability
- EXPERIMENTAL MODEL AND SUBJECT DETAILS
 - Mice
 - Bacterial strains
- METHOD DETAILS
 - Adoptive Transfer of T Cells into Lymphopenic Mice
 - *In Vivo* Activation and Immunization
 - T Cell Activation
 - *In Vitro* T_{reg} Proliferation Inhibition Assay
 - Cell Preparation and Flow Cytometry
 - Bromodeoxyuridine Incorporation Assay
 - Gene Expression Analysis
 - NanoString Analysis
 - RNA-Seq and Transcriptome Analysis
 - Chromatin Immunoprecipitation (ChIP)
- QUANTIFICATION AND STATISTICAL ANALYSIS

SUPPLEMENTAL INFORMATION

Supplemental Information can be found online at <https://doi.org/10.1016/j.celrep.2020.108219>.

ACKNOWLEDGMENTS

This work was supported by funding from NIH (R21 AI097600 to P.K.).

AUTHOR CONTRIBUTIONS

P.K. conceived, supervised, and obtained funding. L.M.B., C.M., M.K., and Y.J. performed experiments. M.P. and G.R. performed statistical analysis. P.K. wrote the original draft, and L.M.B., P.M., L.L., and M.K. reviewed and edited manuscript.

Figure 7. BMPR1 α Controls Epigenetic Changes Associated with the Maturation and Stability of T_{reg} Cells and Differentiation of iT_{reg} and Th17 Cells

(A and B) RNA-seq and qRT-PCR analysis of *KDM6B* mRNA expression in activated and iT_{reg} cells (A) and sorted T_{reg} cells (B) from WT and BMPR1 α ^{TR-/-} mice. Data are means \pm SD pooled from three independent RNA-seq samples or three sorts of T_{reg} cells.

(C) qRT-PCR analysis of *FOXP3* mRNA expression in T_{reg} cells sorted from WT (left panel) and BMPR1 α ^{TR-/-} (right panel) mice and stimulated with plate-bound anti-CD3/anti-CD28 antibodies in the presence of IL-2 and in the absence (Ctrl) or presence of KDM6B inhibitor (GSK-J4, 600 nM).

(D) qRT-PCR analysis of *FOXP3* mRNA expression and flow cytometry analysis of Foxp3^{GFP} in naive CD4⁺ T cells sorted from WT and BMPR1 α ^{TR-/-} mice and stimulated in iT_{reg} polarizing conditions in the absence or presence of GSK-J4. Data are means \pm SD pooled from three independent activations.

(E) qRT-PCR analysis of *RORC* mRNA expression and flow cytometry analysis of IL-17 in naive CD4⁺ T cells sorted from WT and BMPR1 α ^{TR-/-} mice and stimulated in Th17 polarizing conditions in the absence or presence of GSK-J4. Data are means \pm SD pooled from three independent activations. *p < 0.05, **p < 0.01, ***p < 0.001, ****p < 0.0001 as determined by Student's t test.

(F) Analysis of relative abundance of *CDKN1A*, *FOXP3*, and *RORC* gene regions associated with tri-methylated histone H3. T_{reg} cells were sorted from WT and BMPR1 α ^{TR-/-} mice and methylation of chromatin associated with *CDKN1A*, *FOXP3*, and *RORC* genes was examined by chromatin immunoprecipitation with anti-H3K27me3 specific antibody and quantitative PCR. Two sets of experimental WT and BMPR1 α ^{TR-/-} mice were analyzed.

DECLARATION OF INTERESTS

The authors have declared no competing interests.

Received: September 10, 2019

Revised: July 28, 2020

Accepted: September 10, 2020

Published: October 6, 2020

REFERENCES

Abbas, A.K., Benoist, C., Bluestone, J.A., Campbell, D.J., Ghosh, S., Hori, S., Jiang, S., Kuchroo, V.K., Mathis, D., Roncarolo, M.G., et al. (2013). Regulatory T cells: recommendations to simplify the nomenclature. *Nat. Immunol.* *14*, 307–308.

Arias, C.F., Ballesteros-Tato, A., García, M.I., Martín-Caballero, J., Flores, J.M., Martínez-A, C., and Balomenos, D. (2007). p21CIP1/WAF1 controls proliferation of activated/memory T cells and affects homeostasis and memory T cell responses. *J. Immunol.* *178*, 2296–2306.

Bailey-Bucktrout, S.L., Martínez-Llordella, M., Zhou, X., Anthony, B., Rosenthal, W., Luche, H., Fehling, H.J., and Bluestone, J.A. (2013). Self-antigen-driven activation induces instability of regulatory T cells during an inflammatory autoimmune response. *Immunity* *39*, 949–962.

Belkaid, Y., Piccirillo, C.A., Mendez, S., Shevach, E.M., and Sacks, D.L. (2002). CD4+CD25+ regulatory T cells control *Leishmania* major persistence and immunity. *Nature* *420*, 502–507.

Beriou, G., Costantino, C.M., Ashley, C.W., Yang, L., Kuchroo, V.K., Baecher-Allan, C., and Hafler, D.A. (2009). IL-17-producing human peripheral regulatory T cells retain suppressive function. *Blood* *113*, 4240–4249.

Bettini, M.L., Pan, F., Bettini, M., Finkelstein, D., Rehg, J.E., Floess, S., Bell, B.D., Ziegler, S.F., Huehn, J., Pardoll, D.M., and Vignali, D.A. (2012). Loss of epigenetic modification driven by the Foxp3 transcription factor leads to regulatory T cell insufficiency. *Immunity* *36*, 717–730.

Bilate, A.M., and Lafaille, J.J. (2012). Induced CD4+Foxp3+ regulatory T cells in immune tolerance. *Annu. Rev. Immunol.* *30*, 733–758.

Blatner, N.R., Mulcahy, M.F., Dennis, K.L., Scholtens, D., Bentrem, D.J., Phillips, J.D., Ham, S., Sandall, B.P., Khan, M.W., Mahvi, D.M., et al. (2012). Expression of ROR γ t marks a pathogenic regulatory T cell subset in human colon cancer. *Sci. Transl. Med.* *4*, 164ra159.

Bragdon, B., Moseychuk, O., Saldanha, S., King, D., Julian, J., and Nohe, A. (2011). Bone morphogenetic proteins: a critical review. *Cell. Signal.* *23*, 609–620.

Browning, L.M., Pietrzak, M., Kuczma, M., Simms, C.P., Kurczewska, A., Refugia, J.M., Lowery, D.J., Rempala, G., Gutkin, D., Ignatowicz, L., et al. (2018). TGF- β -mediated enhancement of T_H17 cell generation is inhibited by bone morphogenetic protein receptor 1 α signaling. *Sci. Signal.* *11*, eaar2125.

Carreira, A.C., Alves, G.G., Zambuzzi, W.F., Sogayar, M.C., and Granjeiro, J.M. (2014). Bone Morphogenetic Proteins: structure, biological function and therapeutic applications. *Arch. Biochem. Biophys.* *561*, 64–73.

Chen, W., and Ten Dijke, P. (2016). Immunoregulation by members of the TGF β superfamily. *Nat. Rev. Immunol.* *16*, 723–740.

Chen, W., Jin, W., Hardegen, N., Lei, K.J., Li, L., Marinos, N., McGrady, G., and Wahl, S.M. (2003). Conversion of peripheral CD4+CD25- naive T cells to CD4+CD25+ regulatory T cells by TGF-beta induction of transcription factor Foxp3. *J. Exp. Med.* *198*, 1875–1886.

Cheng, G., Yuan, X., Tsai, M.S., Podack, E.R., Yu, A., and Malek, T.R. (2012). IL-2 receptor signaling is essential for the development of Klrp1+ terminally differentiated T regulatory cells. *J. Immunol.* *189*, 1780–1791.

Chou, W.C., Cheng, A.L., Brotto, M., and Chuang, C.Y. (2014). Visual gene-network analysis reveals the cancer gene co-expression in human endometrial cancer. *BMC Genomics* *15*, 300.

Ciofani, M., Madar, A., Galan, C., Sellars, M., Mace, K., Pauli, F., Agarwal, A., Huang, W., Parkhurst, C.N., Muratet, M., et al. (2012). A validated regulatory network for Th17 cell specification. *Cell* *151*, 289–303.

Cobbold, S.P., Castejon, R., Adams, E., Zelenika, D., Graca, L., Humm, S., and Waldmann, H. (2004). Induction of foxP3+ regulatory T cells in the periphery of T cell receptor transgenic mice tolerized to transplants. *J. Immunol.* *172*, 6003–6010.

Collins, J.W., Keeney, K.M., Crepin, V.F., Rathinam, V.A., Fitzgerald, K.A., Finlay, B.B., and Frankel, G. (2014). *Citrobacter rodentium*: infection, inflammation and the microbiota. *Nat. Rev. Microbiol.* *12*, 612–623.

Crepin, V.F., Collins, J.W., Habibzay, M., and Frankel, G. (2016). *Citrobacter rodentium* mouse model of bacterial infection. *Nat. Protoc.* *11*, 1851–1876.

Curotto de Lafaille, M.A., Kutchukhidze, N., Shen, S., Ding, Y., Yee, H., and Lafaille, J.J. (2008). Adaptive Foxp3+ regulatory T cell-dependent and -independent control of allergic inflammation. *Immunity* *29*, 114–126.

Curran, M.A., Geiger, T.L., Montalvo, W., Kim, M., Reiner, S.L., Al-Shamkhani, A., Sun, J.C., and Allison, J.P. (2013). Systemic 4-1BB activation induces a novel T cell phenotype driven by high expression of Eomesodermin. *J. Exp. Med.* *210*, 743–755.

Deaglio, S., Dwyer, K.M., Gao, W., Friedman, D., Usheva, A., Erat, A., Chen, J.F., Enjyoji, K., Linden, J., Oukka, M., et al. (2007). Adenosine generation catalyzed by CD39 and CD73 expressed on regulatory T cells mediates immune suppression. *J. Exp. Med.* *204*, 1257–1265.

Do, J., Kim, D., Kim, S., Valentin-Torres, A., Dvorina, N., Jang, E., Nagarajavel, V., DeSilva, T.M., Li, X., Ting, A.H., et al. (2017). Treg-specific IL-27R α deletion uncovers a key role for IL-27 in Treg function to control autoimmunity. *Proc. Natl. Acad. Sci. USA* *114*, 10190–10195.

Dominguez-Villar, M., and Hafler, D.A. (2018). Regulatory T cells in autoimmune disease. *Nat. Immunol.* *19*, 665–673.

Fessler, J., Raicht, A., Husic, R., Ficjan, A., Schwarz, C., Duftner, C., Schwinger, W., Graninger, W.B., Stradner, M.H., and Dejaco, C. (2017). Novel Senescent Regulatory T-Cell Subset with Impaired Suppressive Function in Rheumatoid Arthritis. *Front. Immunol.* *8*, 300.

Fletcher, J.M., Lonergan, R., Costelloe, L., Kinsella, K., Moran, B., O'Farrelly, C., Tubridy, N., and Mills, K.H. (2009). CD39+Foxp3+ regulatory T Cells suppress pathogenic Th17 cells and are impaired in multiple sclerosis. *J. Immunol.* *183*, 7602–7610.

Fu, W., Ergun, A., Lu, T., Hill, J.A., Haxhinasto, S., Fassett, M.S., Gazit, R., Adoro, S., Glimcher, L., Chan, S., et al. (2012). A multiply redundant genetic switch 'locks in' the transcriptional signature of regulatory T cells. *Nat. Immunol.* *13*, 972–980.

Gagliani, N., Amezcua Vesely, M.C., Iseppon, A., Brockmann, L., Xu, H., Palm, N.W., de Zoete, M.R., Licona-Limón, P., Paiva, R.S., Ching, T., et al. (2015). Th17 cells transdifferentiate into regulatory T cells during resolution of inflammation. *Nature* *523*, 221–225.

Gao, Y., Tang, J., Chen, W., Li, Q., Nie, J., Lin, F., Wu, Q., Chen, Z., Gao, Z., Fan, H., et al. (2015). Inflammation negatively regulates FOXP3 and regulatory T-cell function via DBC1. *Proc. Natl. Acad. Sci. USA* *112*, E3246–E3254.

Ghoreschi, K., Laurence, A., Yang, X.P., Tato, C.M., McGeachy, M.J., Konkeli, J.E., Ramos, H.L., Wei, L., Davidson, T.S., Bouladoux, N., et al. (2010). Generation of pathogenic T(H)17 cells in the absence of TGF- β signalling. *Nature* *467*, 967–971.

Gratz, I.K., Truong, H.A., Yang, S.H., Maurano, M.M., Lee, K., Abbas, A.K., and Rosenblum, M.D. (2013). Cutting Edge: memory regulatory t cells require IL-7 and not IL-2 for their maintenance in peripheral tissues. *J. Immunol.* *190*, 4483–4487.

Gratz, I.K., Rosenblum, M.D., Maurano, M.M., Paw, J.S., Truong, H.A., Marshak-Rothstein, A., and Abbas, A.K. (2014). Cutting edge: Self-antigen controls the balance between effector and regulatory T cells in peripheral tissues. *J. Immunol.* *192*, 1351–1355.

Guo, J., and Zhou, X. (2015). Regulatory T cells turn pathogenic. *Cell. Mol. Immunol.* *12*, 525–532.

Hager-Theodorides, A.L., Ross, S.E., Sahni, H., Mishina, Y., Furmanski, A.L., and Crompton, T. (2014). Direct BMP2/4 signaling through BMP receptor IA regulates fetal thymocyte progenitor homeostasis and differentiation to CD4+CD8+ double-positive cell. *Cell Cycle* *13*, 324–333.

- Haribhai, D., Williams, J.B., Jia, S., Nickerson, D., Schmitt, E.G., Edwards, B., Ziegelbauer, J., Yassai, M., Li, S.H., Relland, L.M., et al. (2011). A requisite role for induced regulatory T cells in tolerance based on expanding antigen receptor diversity. *Immunity* **35**, 109–122.
- Hill, J.A., Feuerer, M., Tash, K., Haxhinasto, S., Perez, J., Melamed, R., Mathis, D., and Benoist, C. (2007). Foxp3 transcription-factor-dependent and -independent regulation of the regulatory T cell transcriptional signature. *Immunity* **27**, 786–800.
- Hori, S. (2011). Regulatory T cell plasticity: beyond the controversies. *Trends Immunol.* **32**, 295–300.
- Huber, S., Stahl, F.R., Schrader, J., Lüth, S., Presser, K., Carambia, A., Flavell, R.A., Werner, S., Blessing, M., Herkel, J., and Schramm, C. (2009). Activin A promotes the TGF-beta-induced conversion of CD4+CD25- T cells into Foxp3+ induced regulatory T cells. *J. Immunol.* **182**, 4633–4640.
- Huter, E.N., Punkosdy, G.A., Glass, D.D., Cheng, L.I., Ward, J.M., and Shevach, E.M. (2008). TGF-beta-induced Foxp3+ regulatory T cells rescue scurfy mice. *Eur. J. Immunol.* **38**, 1814–1821.
- Ishimura, A., Minehata, K., Terashima, M., Kondoh, G., Hara, T., and Suzuki, T. (2012). Jmjd5, an H3K36me2 histone demethylase, modulates embryonic cell proliferation through the regulation of Cdkn1a expression. *Development* **139**, 749–759.
- Ivanov, I.I., McKenzie, B.S., Zhou, L., Tadokoro, C.E., Lepelley, A., Lafaille, J.J., Cua, D.J., and Littman, D.R. (2006). The orphan nuclear receptor ROR-gamma directs the differentiation program of proinflammatory IL-17+ T helper cells. *Cell* **126**, 1121–1133.
- Josefowicz, S.Z., Lu, L.F., and Rudensky, A.Y. (2012). Regulatory T cells: mechanisms of differentiation and function. *Annu. Rev. Immunol.* **30**, 531–564.
- Jurberg, A.D., Vasconcelos-Fontes, L., and Cotta-de-Almeida, V. (2015). A Tale from TGF-β Superfamily for Thymus Ontogeny and Function. *Front. Immunol.* **6**, 442.
- Kara, E.E., McKenzie, D.R., Bastow, C.R., Gregor, C.E., Fenix, K.A., Ogunniyi, A.D., Paton, J.C., Mack, M., Pombal, D.R., Seillet, C., et al. (2015). CCR2 defines in vivo development and homing of IL-23-driven GM-CSF-producing Th17 cells. *Nat. Commun.* **6**, 8644.
- Kendal, A.R., Chen, Y., Regateiro, F.S., Ma, J., Adams, E., Cobbold, S.P., Hori, S., and Waldmann, H. (2011). Sustained suppression by Foxp3+ regulatory T cells is vital for infectious transplantation tolerance. *J. Exp. Med.* **208**, 2043–2053.
- Komatsu, N., Mariotti-Ferrandiz, M.E., Wang, Y., Malissen, B., Waldmann, H., and Hori, S. (2009). Heterogeneity of natural Foxp3+ T cells: a committed regulatory T-cell lineage and an uncommitted minor population retaining plasticity. *Proc. Natl. Acad. Sci. USA* **106**, 1903–1908.
- Komatsu, N., Okamoto, K., Sawa, S., Nakashima, T., Oh-hora, M., Kodama, T., Tanaka, S., Bluestone, J.A., and Takayanagi, H. (2014). Pathogenic conversion of Foxp3+ T cells into TH17 cells in autoimmune arthritis. *Nat. Med.* **20**, 62–68.
- Konkel, J.E., Zhang, D., Zanvit, P., Chia, C., Zangarile-Murray, T., Jin, W., Wang, S., and Chen, W. (2017). Transforming Growth Factor-β Signaling in Regulatory T Cells Controls T Helper-17 Cells and Tissue-Specific Immune Responses. *Immunity* **46**, 660–674.
- Kuchroo, V.K., Ohashi, P.S., Sartor, R.B., and Vinuesa, C.G. (2012). Dysregulation of immune homeostasis in autoimmune diseases. *Nat. Med.* **18**, 42–47.
- Kuczma, M., Pawlikowska, I., Kopij, M., Podolsky, R., Rempala, G.A., and Kraj, P. (2009a). TCR repertoire and Foxp3 expression define functionally distinct subsets of CD4+ regulatory T cells. *J. Immunol.* **183**, 3118–3129.
- Kuczma, M., Podolsky, R., Garge, N., Daniely, D., Pacholczyk, R., Ignatowicz, L., and Kraj, P. (2009b). Foxp3-deficient regulatory T cells do not revert into conventional effector CD4+ T cells but constitute a unique cell subset. *J. Immunol.* **183**, 3731–3741.
- Kuczma, M., Kurczewska, A., and Kraj, P. (2014). Modulation of bone morphogenetic protein signaling in T-cells for cancer immunotherapy. *J. Immunotoxicol.* **11**, 319–327.
- Landuyt, A.E., Klocke, B.J., Colvin, T.B., Schoeb, T.R., and Maynard, C.L. (2019). Cutting Edge: ICOS-Deficient Regulatory T Cells Display Normal Induction of *Il10* but Readily Downregulate Expression of Foxp3. *J. Immunol.* **202**, 1039–1044.
- Langfelder, P., and Horvath, S. (2008). WGCNA: an R package for weighted correlation network analysis. *BMC Bioinformatics* **9**, 559.
- Lathrop, S.K., Bloom, S.M., Rao, S.M., Nutsch, K., Lio, C.W., Santacruz, N., Peterson, D.A., Stappenbeck, T.S., and Hsieh, C.S. (2011). Peripheral education of the immune system by colonic commensal microbiota. *Nature* **478**, 250–254.
- Lee, P.P., Fitzpatrick, D.R., Beard, C., Jessup, H.K., Lehar, S., Makar, K.W., Pérez-Melgosa, M., Sweetser, M.T., Schlissel, M.S., Nguyen, S., et al. (2001). A critical role for Dnmt1 and DNA methylation in T cell development, function, and survival. *Immunity* **15**, 763–774.
- Levine, A.G., Arvey, A., Jin, W., and Rudensky, A.Y. (2014). Continuous requirement for the TCR in regulatory T cell function. *Nat. Immunol.* **15**, 1070–1078.
- Li, M.O., and Flavell, R.A. (2008). TGF-beta: a master of all T cell trades. *Cell* **134**, 392–404.
- Li, Z., Fei, T., Zhang, J., Zhu, G., Wang, L., Lu, D., Chi, X., Teng, Y., Hou, N., Yang, X., et al. (2012). BMP4 Signaling Acts via dual-specificity phosphatase 9 to control ERK activity in mouse embryonic stem cells. *Cell Stem Cell* **10**, 171–182.
- Liu, Z., Cao, W., Xu, L., Chen, X., Zhan, Y., Yang, Q., Liu, S., Chen, P., Jiang, Y., Sun, X., et al. (2015). The histone H3 lysine-27 demethylase Jmjd3 plays a critical role in specific regulation of Th17 cell differentiation. *J. Mol. Cell Biol.* **7**, 505–516.
- Long, S.A., and Buckner, J.H. (2011). CD4+FOXP3+ T regulatory cells in human autoimmunity: more than a numbers game. *J. Immunol.* **187**, 2061–2066.
- Lu, L., Ma, J., Wang, X., Wang, J., Zhang, F., Yu, J., He, G., Xu, B., Brand, D.D., Horwitz, D.A., et al. (2010). Synergistic effect of TGF-beta superfamily members on the induction of Foxp3+ Treg. *Eur. J. Immunol.* **40**, 142–152.
- Lupar, E., Brack, M., Garnier, L., Laffont, S., Rauch, K.S., Schachtrup, K., Arnold, S.J., Guéry, J.C., and Izcue, A. (2015). Eomesodermin Expression in CD4+ T Cells Restricts Peripheral Foxp3 Induction. *J. Immunol.* **195**, 4742–4752.
- Madireddi, S., Eun, S.Y., Lee, S.W., Nemčovičová, I., Mehta, A.K., Zajonc, D.M., Nishi, N., Niki, T., Hirashima, M., and Croft, M. (2014). Galectin-9 controls the therapeutic activity of 4-1BB-targeting antibodies. *J. Exp. Med.* **211**, 1433–1448.
- Malek, T.R., Yu, A., Vincek, V., Scibelli, P., and Kong, L. (2002). CD4 regulatory T cells prevent lethal autoimmunity in IL-2Rbeta-deficient mice. Implications for the nonredundant function of IL-2. *Immunity* **17**, 167–178.
- Maric, I., Wensveen, T.T., Smoljan, I., Orlic, Z.C., and Bobinac, D. (2012). Bone Morphogenetic Proteins and signaling pathway in Inflammatory Bowel Disease. *Adv. Pathogen. Manage.* Published online January 27, 2012.
- Martin, B., Auffray, C., Delpoux, A., Pommier, A., Durand, A., Charvet, C., Yakonowsky, P., de Boysson, H., Bonilla, N., Audemard, A., et al. (2013). Highly self-reactive naive CD4 T cells are prone to differentiate into regulatory T cells. *Nat. Commun.* **4**, 2209.
- Martínez, V.G., Sacedón, R., Hidalgo, L., Valencia, J., Fernández-Sevilla, L.M., Hernández-López, C., Vicente, A., and Varas, A. (2015). The BMP Pathway Participates in Human Naive CD4+ T Cell Activation and Homeostasis. *PLoS ONE* **10**, e0131453.
- Min, B. (2017). Heterogeneity and Stability in Foxp3+ Regulatory T Cells. *J. Interferon Cytokine Res.* **37**, 386–397.
- Mishina, Y., Suzuki, A., Ueno, N., and Behringer, R.R. (1995). Bmpr encodes a type I bone morphogenetic protein receptor that is essential for gastrulation during mouse embryogenesis. *Genes Dev.* **9**, 3027–3037.
- Mishina, Y., Hanks, M.C., Miura, S., Tallquist, M.D., and Behringer, R.R. (2002). Generation of Bmpr/Alk3 conditional knockout mice. *Genesis* **32**, 69–72.
- Miyao, T., Floess, S., Setoguchi, R., Luche, H., Fehling, H.J., Waldmann, H., Huehn, J., and Hori, S. (2012). Plasticity of Foxp3(+) T cells reflects promiscuous Foxp3 expression in conventional T cells but not reprogramming of regulatory T cells. *Immunity* **36**, 262–275.

- Miyazono, K., Kamiya, Y., and Morikawa, M. (2010). Bone morphogenetic protein receptors and signal transduction. *J. Biochem.* *147*, 35–51.
- Mombaerts, P., Clarke, A.R., Rudnicki, M.A., Iacomini, J., Itohara, S., Lafaille, J.J., Wang, L., Ichikawa, Y., Jaenisch, R., Hooper, M.L., et al. (1992). Mutations in T-cell antigen receptor genes alpha and beta block thymocyte development at different stages. *Nature* *360*, 225–231.
- Morikawa, H., and Sakaguchi, S. (2014). Genetic and epigenetic basis of Treg cell development and function: from a FoxP3-centered view to an epigenome-defined view of natural Treg cells. *Immunol. Rev.* *259*, 192–205.
- Muñoz-Espin, D., Cañamero, M., Maraver, A., Gómez-López, G., Contreras, J., Murillo-Cuesta, S., Rodríguez-Baeza, A., Varela-Nieto, I., Ruberte, J., Collado, M., and Serrano, M. (2013). Programmed cell senescence during mammalian embryonic development. *Cell* *155*, 1104–1118.
- Ntzachristos, P., Tsirigos, A., Welstead, G.G., Trimarchi, T., Bakogianni, S., Xu, L., Loizou, E., Holmfeldt, L., Strikoudis, A., King, B., et al. (2014). Contrasting roles of histone 3 lysine 27 demethylases in acute lymphoblastic leukaemia. *Nature* *514*, 513–517.
- Obata, Y., Furusawa, Y., Endo, T.A., Sharif, J., Takahashi, D., Atarashi, K., Nakayama, M., Onawa, S., Fujimura, Y., Takahashi, M., et al. (2014). The epigenetic regulator Uhrf1 facilitates the proliferation and maturation of colonic regulatory T cells. *Nat. Immunol.* *15*, 571–579.
- Qin, L., Zhou, Y.C., Wu, H.J., Zhuo, Y., Wang, Y.P., Si, C.Y., and Qin, Y.M. (2017). Notch Signaling Modulates the Balance of Regulatory T Cells and T Helper 17 Cells in Patients with Chronic Hepatitis C. *DNA Cell Biol.* *36*, 311–320.
- Radhakrishnan, S., Cabrera, R., Schenk, E.L., Nava-Parada, P., Bell, M.P., Van Keulen, V.P., Marler, R.J., Felts, S.J., and Pease, L.R. (2008). Reprogrammed FoxP3+ T regulatory cells become IL-17+ antigen-specific autoimmune effectors in vitro and in vivo. *J. Immunol.* *181*, 3137–3147.
- Ren, J., and Li, B. (2017). The Functional Stability of FOXP3 and ROR γ t in Treg and Th17 and Their Therapeutic Applications. *Adv. Protein Chem. Struct. Biol.* *107*, 155–189.
- Rong, H., Shen, H., Xu, Y., and Yang, H. (2016). Notch signalling suppresses regulatory T-cell function in murine experimental autoimmune uveitis. *Immunology* *149*, 447–459.
- Rosenblum, M.D., Gratz, I.K., Paw, J.S., Lee, K., Marshak-Rothstein, A., and Abbas, A.K. (2011). Response to self antigen imprints regulatory memory in tissues. *Nature* *480*, 538–542.
- Rubtsov, Y.P., Niec, R.E., Josefowicz, S., Li, L., Darce, J., Mathis, D., Benoist, C., and Rudensky, A.Y. (2010). Stability of the regulatory T cell lineage in vivo. *Science* *329*, 1667–1671.
- Saito, T., Nishikawa, H., Wada, H., Nagano, Y., Sugiyama, D., Atarashi, K., Maeda, Y., Hamaguchi, M., Ohkura, N., Sato, E., et al. (2016). Two FOXP3(+) CD4(+) T cell subpopulations distinctly control the prognosis of colorectal cancers. *Nat. Med.* *22*, 679–684.
- Sakaguchi, S., Miyara, M., Costantino, C.M., and Hafler, D.A. (2010). FOXP3+ regulatory T cells in the human immune system. *Nat. Rev. Immunol.* *10*, 490–500.
- Salminen, A., Kaarniranta, K., Hiltunen, M., and Kauppinen, A. (2014). Histone demethylase Jumonji D3 (JMJD3/KDM6B) at the nexus of epigenetic regulation of inflammation and the aging process. *J. Mol. Med. (Berl.)* *92*, 1035–1043.
- Sawant, D.V., and Vignali, D.A. (2014). Once a Treg, always a Treg? *Immunol. Rev.* *259*, 173–191.
- Selma Dagtas, A., and Gilbert, K.M. (2010). p21(Cip1) up-regulated during histone deacetylase inhibitor-induced CD4(+) T-cell anergy selectively associates with mitogen-activated protein kinases. *Immunology* *129*, 589–599.
- Shannon, P., Markiel, A., Ozier, O., Baliga, N.S., Wang, J.T., Ramage, D., Amin, N., Schwikowski, B., and Ideker, T. (2003). Cytoscape: a software environment for integrated models of biomolecular interaction networks. *Genome Res.* *13*, 2498–2504.
- Sharma, M.D., Huang, L., Choi, J.H., Lee, E.J., Wilson, J.M., Lemos, H., Pan, F., Blazar, B.R., Pardoll, D.M., Mellor, A.L., et al. (2013). An inherently bifunctional subset of Foxp3+ T helper cells is controlled by the transcription factor eos. *Immunity* *38*, 998–1012.
- Shevach, E.M. (2018). Foxp3+ T Regulatory Cells: Still Many Unanswered Questions—A Perspective After 20 Years of Study. *Front. Immunol.* *9*, 1048.
- Shih, H.Y., Sciumè, G., Poholek, A.C., Vahedi, G., Hirahara, K., Villarino, A.V., Bonelli, M., Bosselut, R., Kanno, Y., Muljo, S.A., and O’Shea, J.J. (2014). Transcriptional and epigenetic networks of helper T and innate lymphoid cells. *Immunol. Rev.* *261*, 23–49.
- So, T., Lee, S.W., and Croft, M. (2008). Immune regulation and control of regulatory T cells by OX40 and 4-1BB. *Cytokine Growth Factor Rev.* *19*, 253–262.
- Takabayashi, H., Shinohara, M., Mao, M., Phaosawasdi, P., El-Zaatari, M., Zhang, M., Ji, T., Eaton, K.A., Dang, D., Kao, J., et al. (2014). Anti-inflammatory activity of bone morphogenetic protein signaling pathways in stomachs of mice. *Gastroenterology* *147*, 396–406.
- Thornton, A.M., Donovan, E.E., Piccirillo, C.A., and Shevach, E.M. (2004). Cutting edge: IL-2 is critically required for the in vitro activation of CD4+CD25+ T cell suppressor function. *J. Immunol.* *172*, 6519–6523.
- Toomer, K.H., Yuan, X., Yang, J., Dee, M.J., Yu, A., and Malek, T.R. (2016). Developmental Progression and Interrelationship of Central and Effector Regulatory T Cell Subsets. *J. Immunol.* *196*, 3665–3676.
- Trapnell, C., Roberts, A., Goff, L., Pertea, G., Kim, D., Kelley, D.R., Pimentel, H., Salzberg, S.L., Rinn, J.L., and Pachter, L. (2012). Differential gene and transcript expression analysis of RNA-seq experiments with TopHat and Cufflinks. *Nat. Protoc.* *7*, 562–578.
- Tripathi, S., Pohl, M.O., Zhou, Y., Rodriguez-Frandsen, A., Wang, G., Stein, D.A., Moulton, H.M., DeJesus, P., Che, J., Mulder, L.C., et al. (2015). Meta- and Orthogonal Integration of Influenza “OMICs” Data Defines a Role for UBR4 in Virus Budding. *Cell Host Microbe* *18*, 723–735.
- Vahl, J.C., Drees, C., Heger, K., Heink, S., Fischer, J.C., Nedjic, J., Ohkura, N., Morikawa, H., Poeck, H., Schallenberg, S., et al. (2014). Continuous T cell receptor signals maintain a functional regulatory T cell pool. *Immunity* *41*, 722–736.
- Varas, A., Hager-Theodorides, A.L., Sacedón, R., Vicente, A., Zapata, A.G., and Crompton, T. (2003). The role of morphogens in T-cell development. *Trends Immunol.* *24*, 197–206.
- Varas, A., Valencia, J., Lavocat, F., Martínez, V.G., Thiam, N.N., Hidalgo, L., Fernández-Sevilla, L.M., Sacedón, R., Vicente, A., and Miossec, P. (2015). Blockade of bone morphogenetic protein signaling potentiates the pro-inflammatory phenotype induced by interleukin-17 and tumor necrosis factor- α combination in rheumatoid synoviocytes. *Arthritis Res. Ther.* *17*, 192.
- Voo, K.S., Wang, Y.H., Santori, F.R., Boggiano, C., Wang, Y.H., Arima, K., Bover, L., Hanabuchi, S., Khalili, J., Marinova, E., et al. (2009). Identification of IL-17-producing FOXP3+ regulatory T cells in humans. *Proc. Natl. Acad. Sci. USA* *106*, 4793–4798.
- Wan, Y.Y., and Flavell, R.A. (2007). Regulatory T-cell functions are subverted and converted owing to attenuated Foxp3 expression. *Nature* *445*, 766–770.
- Wang, D., Quiros, J., Mahuron, K., Pai, C.C., Ranzani, V., Young, A., Silveria, S., Harwin, T., Abnousian, A., Pagani, M., et al. (2018). Targeting EZH2 Reprograms Intratumoral Regulatory T Cells to Enhance Cancer Immunity. *Cell Rep.* *23*, 3262–3274.
- Weinmann, A.S. (2014). Roles for helper T cell lineage-specifying transcription factors in cellular specialization. *Adv. Immunol.* *124*, 171–206.
- Wing, J.B., Tanaka, A., and Sakaguchi, S. (2019). Human FOXP3+ Regulatory T Cell Heterogeneity and Function in Autoimmunity and Cancer. *Immunity* *50*, 302–316.
- Wu, M.Y., and Hill, C.S. (2009). Tgf-beta superfamily signaling in embryonic development and homeostasis. *Dev. Cell* *16*, 329–343.
- Xiao, X.Y., Li, Y.T., Jiang, X., Ji, X., Lu, X., Yang, B., Wu, L.J., Wang, X.H., Guo, J.B., Zhao, L.D., et al. (2020). EZH2 deficiency attenuates Treg differentiation in rheumatoid arthritis. *J. Autoimmun.* *108*, 102404.
- Xiong, Y., Khanna, S., Grzenda, A.L., Sarmento, O.F., Svingsen, P.A., Lomber, G.A., Urrutia, R.A., and Faubion, W.A., Jr. (2012). Polycomb antagonizes p300/

- CREB-binding protein-associated factor to silence FOXP3 in a Kruppel-like factor-dependent manner. *J. Biol. Chem.* *287*, 34372–34385.
- Yang, X.O., Nurieva, R., Martinez, G.J., Kang, H.S., Chung, Y., Pappu, B.P., Shah, B., Chang, S.H., Schluns, K.S., Watowich, S.S., et al. (2008a). Molecular antagonism and plasticity of regulatory and inflammatory T cell programs. *Immunity* *29*, 44–56.
- Yang, Y., Xu, J., Niu, Y., Bromberg, J.S., and Ding, Y. (2008b). T-bet and eomesodermin play critical roles in directing T cell differentiation to Th1 versus Th17. *J. Immunol.* *181*, 8700–8710.
- Yang, B.H., Hagemann, S., Mamareli, P., Lauer, U., Hoffmann, U., Beckstette, M., Föhse, L., Prinz, I., Pezoldt, J., Suerbaum, S., et al. (2016). Foxp3(+) T cells expressing ROR γ t represent a stable regulatory T-cell effector lineage with enhanced suppressive capacity during intestinal inflammation. *Mucosal Immunol.* *9*, 444–457.
- Ying, Q.L., Nichols, J., Chambers, I., and Smith, A. (2003). BMP induction of Id proteins suppresses differentiation and sustains embryonic stem cell self-renewal in collaboration with STAT3. *Cell* *115*, 281–292.
- Yosef, N., Shalek, A.K., Gaublomme, J.T., Jin, H., Lee, Y., Awasthi, A., Wu, C., Karwacz, K., Xiao, S., Jorgolli, M., et al. (2013). Dynamic regulatory network controlling TH17 cell differentiation. *Nature* *496*, 461–468.
- Yoshioka, Y., Ono, M., Osaki, M., Konishi, I., and Sakaguchi, S. (2012). Differential effects of inhibition of bone morphogenic protein (BMP) signalling on T-cell activation and differentiation. *Eur. J. Immunol.* *42*, 749–759.
- Yu, A., Zhu, L., Altman, N.H., and Malek, T.R. (2009). A low interleukin-2 receptor signaling threshold supports the development and homeostasis of T regulatory cells. *Immunity* *30*, 204–217.
- Zeisberg, M., Hanai, J., Sugimoto, H., Mammoto, T., Charytan, D., Strutz, F., and Kalluri, R. (2003). BMP-7 counteracts TGF-beta1-induced epithelial-to-mesenchymal transition and reverses chronic renal injury. *Nat. Med.* *9*, 964–968.
- Zhang, B., and Horvath, S. (2005). A general framework for weighted gene co-expression network analysis. *Stat. Appl. Genet. Mol. Biol.* *4*, Article17.
- Zhao, W., Li, Q., Ayers, S., Gu, Y., Shi, Z., Zhu, Q., Chen, Y., Wang, H.Y., and Wang, R.F. (2013). Jmjd3 inhibits reprogramming by upregulating expression of INK4a/Arf and targeting PHF20 for ubiquitination. *Cell* *152*, 1037–1050.
- Zhou, X., Jeker, L.T., Fife, B.T., Zhu, S., Anderson, M.S., McManus, M.T., and Bluestone, J.A. (2008). Selective miRNA disruption in T reg cells leads to uncontrolled autoimmunity. *J. Exp. Med.* *205*, 1983–1991.
- Zhou, L., Chong, M.M., and Littman, D.R. (2009a). Plasticity of CD4+ T cell lineage differentiation. *Immunity* *30*, 646–655.
- Zhou, X., Bailey-Bucktrout, S.L., Jeker, L.T., Penaranda, C., Martínez-Llordella, M., Ashby, M., Nakayama, M., Rosenthal, W., and Bluestone, J.A. (2009b). Instability of the transcription factor Foxp3 leads to the generation of pathogenic memory T cells in vivo. *Nat. Immunol.* *10*, 1000–1007.
- Zhou, Y., Zhou, B., Pache, L., Chang, M., Khodabakhshi, A.H., Tanaseichuk, O., Benner, C., and Chanda, S.K. (2019). Metascape provides a biologist-oriented resource for the analysis of systems-level datasets. *Nat. Commun.* *10*, 1523.

STAR★METHODS

KEY RESOURCES TABLE

REAGENT or RESOURCE	SOURCE	IDENTIFIER
Antibodies		
Anti-Mouse CD3e (145-2C11)	BD Biosciences	Cat# 553058; RRID: AB_394591
Anti-Mouse CD28 (37.51)	BD Biosciences	Cat# 553295; RRID: AB_394764
Anti-Mouse CD4-PE (GK1.5)	BD Biosciences	Cat# 553730, RRID:AB_395014
Anti-Mouse CD4-PE-Cy5 (GK1.5)	Thermo Fisher Scientific	Cat# 15-0041-82, RRID:AB_468695
Anti-Mouse CD4-APC (GK1.5)	BD Biosciences	Cat# 553051, RRID:AB_398528
Anti-Mouse CD4-PECy7 (GK1.5)	Thermo Fisher Scientific	Cat# 25-0041-82, RRID:AB_469576
Anti-Mouse CD4-APC-Cy7 (GK1.5)	BD Biosciences	Cat# 552051, RRID:AB_394331
Anti-Mouse CD44-PE-Cy7 (IM7)	BD Biosciences	Cat# 560569, RRID:AB_1727484
Anti-Mouse CD44-PE-Cy5 (IM7)	BD Biosciences	Cat# 553135, RRID:AB_394650
Anti-Mouse CD44-PE (IM7)	BioLegend	Cat# 103008, RRID:AB_312959
Anti-Mouse CD62L-APC-Cy7 (MEL-14)	BD Bioscience	Cat# 560514, RRID:AB_10611861
Anti-Mouse CD45.1-BV421 (A20)	BD Bioscience	Cat# 563983, RRID:AB_2738523
Anti-Mouse CD45.2-APC-Cy7 (104)	BD Bioscience	Cat# 560694, RRID:AB_1727492
Anti-Mouse CD45.2-V500 (104)	BD Bioscience	Cat# 562129, RRID:AB_10897142
Anti-Mouse CD25-PE-Cy7 (PC61)	BD Bioscience	Cat# 561780, RRID:AB_10893596
Anti-Mouse CD25-V450 (PC61)	BD Bioscience	Cat# 561257, RRID:AB_10611871
Anti-Mouse CD137 (4-1BB)-Biotin (17B5)	BioLegend	Cat# 106104, RRID:AB_313241
Anti-Mouse CD278 (ICOS)-PE-Cy5 (15F9)	BioLegend	Cat# 107708, RRID:AB_313337
Anti-Mouse Klrp-1-Biotin (2F1)	BD Bioscience	Cat# 550863, RRID:AB_393931
Anti-Mouse CD127 (IL-7Ra)-PE-Cy5 (A7R34)	BioLegend	Cat# 135015, RRID:AB_1937262
Anti-Mouse CD8a-Biotin (53-6.7)	BD Bioscience	Cat# 553029, RRID:AB_394567
Anti-Mouse CD45R (B220)-Biotin (RA3-6B2)	BioLegend	Cat# 103204, RRID:AB_312989
Anti-Mouse CD11b-Biotin (M1/70)	BioLegend	Cat# 101204, RRID:AB_312787
Anti-Mouse CD11c-Biotin (HL3)	BD Bioscience	Cat# 553800, RRID:AB_395059
Anti-Mouse TER-119-Biotin (TER-119)	BioLegend	Cat# 116204, RRID:AB_313705
Anti-Mouse CD49b-Biotin (DX5)	BioLegend	Cat# 108904, RRID:AB_313411
Anti-Mouse CD196 (CCR6)-PE (29-2L17)	BioLegend	Cat# 129803, RRID:AB_1279139
Anti-Mouse CD45/B220-Biotin (RA3-6B2)	BioLegend	Cat# 103204, RRID:AB_312988
Anti-Mouse IL-17a-PE (TC11-18H10)	BD Bioscience	Cat# 559502, RRID:AB_397256
Anti-Mouse RORgt-PE (Q31-378)	BD Bioscience	Cat# 562607, RRID:AB_11153137
Anti-Mouse IFN-gamma-APC (XMG1.2)	BD Bioscience	Cat# 554413, RRID:AB_398551
Anti-Mouse IL23R-PE (3C9)	BD Bioscience	Cat# 562468, RRID:AB_11154593
Anti-Mouse CD39-Biotin (5F2)	BioLegend	Cat# 135704, RRID:AB_2099920
Anti-Mouse CD279 (PD-1)-PE-Cy7 (29F.1A12)	BioLegend	Cat# 135215, RRID:AB_10696422
Anti-Mouse TIGIT-PE (1G9)	BioLegend	Cat# 142103, RRID:AB_10895760
Anti-BrdU-PE (3D4)	BioLegend	Cat# 364116, RRID:AB_2814317
Streptavidin-V500	BD Biosciences	Cat# 561419, RRID:AB_10611863
Anti-H3K27me3 antibody	Cell Signaling	Cat# 9733; RRID:AB_2616029
Chemicals, Peptides, and Recombinant Proteins		
Lipopolysaccharide from <i>Escherichia coli</i> O111:B4	Sigma	Cat# L4391
Complete Freud's Adjuvant	Sigma	Cat# F5881
Recombinant Murine IL-2	PeproTech	Cat# 212-12
Recombinant Murine IL-6	PeproTech	Cat# 216-16
Recombinant Human TGF-β1	PeproTech	Cat# 100-21
GSK J4	Tocris	Cat# 4594

(Continued on next page)

Continued

REAGENT or RESOURCE	SOURCE	IDENTIFIER
Thymidine	Moravek Inc.	Cat# MT-6036
PMA	Sigma	Cat# P8139
Ionomycin	Sigma	Cat# I0634
Concanavalin A	Sigma	Cat# C5275
BrdU	Sigma	Cat# B5002
eFluor-670	Thermo Fisher Scientific	Cat# 50-246-095
BD IMag streptavidin magnetic beads	BD Biosciences	Cat# 557812
DNase I	Sigma	Cat# 11284932001
Critical Commercial Assays		
BD Cytotfix/Cytoperm Plus Fixation/Permeabilization Solution Kit with BD GolgiPlug (Brefeldin A)	BD Bioscience	Cat# 555028
eBioscience Foxp3/Transcription Factor Staining Buffer Set	Thermo Fisher Scientific	Cat# 00-5523-00
PureLink® RNA Mini kit	Thermo Fisher Scientific	Cat# 12183018A
RNeasy Plus Mini Kit	QIAGEN	Cat# 74136
EZ-CHIP chromatin immunoprecipitation kit	Millipore	Cat# 17-371
TaqMan® Universal Master Mix II	Thermo Fisher Scientific	Cat# 4440043
Power Sybr Green PCR Master Mix	Thermo Fisher Scientific	Cat# 4368577
SuperScript IV First-Strand Synthesis System	Thermo Fisher Scientific	Cat# 18091050
GoTaq DNA polymerase with buffer	Promega	Cat# M3008
Deposited Data		
RNA-seq	This paper	GEO: GSE103124
Experimental Models: Organisms/Strains		
Mouse: <i>Foxp3^{GFP+}</i> (wild-type)	The Jackson Laboratory	JAX, Stock#: 023800
Mouse: <i>Tcra^{tm1Mom}</i>	The Jackson Laboratory	JAX, Stock#: 002116
Mouse: <i>BMPR1α</i> conditional knockout	Gift from Dr. P. Thistlethwaite, UCSD	NA
Mouse: <i>BMPR1α^{TR-}</i>	This paper	NA
Mouse: <i>BMPR1α^{T-}</i>	This paper	NA
Mouse <i>Foxp3^{creGFP+}</i>	The Jackson Laboratory	JAX, Stock#: 023161
Mouse CD4-cre	Taconic	Model#: 4196
Citrobacter rodentium	Gift from Dr. T. Denning, GSU	NA
Oligonucleotides		
Foxp3 (Mm00475157_g1)	Thermo Fisher Scientific	Cat# 4331182
Rorc (Mm01261022_m1)	Thermo Fisher Scientific	Cat# 4331182
Kdm6b (Mm01332680_m1)	Thermo Fisher Scientific	Cat# 4331182
BMPR1 α (Mm00477650_m1)	Thermo Fisher Scientific	Cat# 4331182
IL-10 (Mm00439614_m1)	Thermo Fisher Scientific	Cat# 4331182
Actb (Mm01205647_g1)	Thermo Fisher Scientific	Cat# 4331182
Oligonucleotide sequences for ChIP and conventional PCR analyses are listed in Table S4		
Software and Algorithms		
FlowJo v10	Tree Star, Inc.	https://www.flowjo.com/
nSolver Analysis	nanoString, Inc.	https://www.nanostring.com/products/analysis-software/nsolver
Tophat2	Johns Hopkins University Center for Computational Biology	http://ccb.jhu.edu/software/tophat/index.shtml
Cufflinks 2.1.1	University of Washington	http://cole-trapnell-lab.github.io/cufflinks/
Metascape	Metascape web site	http://metascape.org
R	R	https://www.r-project.org/
Cytoscape	NIGMS and NRNB	https://cytoscape.org/

RESOURCE AVAILABILITY

Lead Contact

Further information and resource requests should be directed to and will be fulfilled by the Lead Contact, Piotr Kraj (pkraj@odu.edu).

Materials Availability

Mouse lines generated in this study are available from the corresponding author.

Data and Code Availability

The accession number for the sequencing data for RNA-seq reported in this paper and submitted to GEO is GSE103124.

EXPERIMENTAL MODEL AND SUBJECT DETAILS

Mice

BMPR1 α ^{TR-} mice were generated by crossing *BMPR1 α* conditional knockout mice with mice expressing creGFP fusion protein controlled by FOXP3 gene regulatory sequences and *Foxp3^{GFP}* reporter mice (Kuczma et al., 2009b; Mishina et al., 1995; Zhou et al., 2008). *BMPR1 α ^{T-}* mice were generated by crossing *BMPR1 α* conditional knockout mice with mice expressing CD4cre and *Foxp3^{GFP}* reporter (Lee et al., 2001; Mishina et al., 2002). TCR α chain knockout (TCR α ⁻) mice were purchased from Jackson Laboratory (Mombaerts et al., 1992). All mice were on the C57BL6 genetic background. Mice were bred and housed in specific pathogen-free conditions in the animal facility of Old Dominion University. Both female and male mice were used in experiments and we have not observed any difference in T cell development and activation between sexes. Unless indicated, mice were 6 to 12 weeks old. All experiments were conducted in accordance with NIH guidelines for the use of live animals and were approved by the IACUC and IBC of the Old Dominion University.

Bacterial strains

Citrobacter rodentium was used to induce mucosal inflammation (Crepin et al., 2016). For inoculations, bacteria were grown overnight in L broth, diluted with PBS to an optical density of 1.7 at 600 nm and delivered to mice via oral gavage in a 100 μ L volume containing 1.5×10^7 CFU.

METHOD DETAILS

Adoptive Transfer of T Cells into Lymphopenic Mice

CD4⁺Foxp3^{GFP^{high}} (Ly5.2⁺) cells from *BMPR1 α ^{TR-}* mice, CD4⁺Foxp3^{GFP} (Ly5.1⁺Ly5.2⁺) and naive (CD44^{low}CD62L^{high}) (Ly5.1⁺) CD4⁺ T cells from wild-type mice were flow sorted, mixed, and used for adoptive transfer. Total of 5×10^5 cells of CD4⁺Foxp3^{GFP^{high}} cells from *BMPR1 α ^{TR-}* mice and CD4⁺Foxp3^{GFP} and naive T cells from wild-type mice were co-transferred i.v. into TCR α ⁻ mice. Cells proportions, mixed at a ratio of 1:0.15:0.15, were analyzed prior to transfer using Ly5.1 (CD45.1) and Ly5.2 (CD45.2) staining. Mice were monitored for 6 weeks at which time they were sacrificed and mesenteric lymph nodes were isolated and analyzed. For single T_{reg} cell transfer, CD4⁺Foxp3^{GFP⁺} T cells were flow sorted from wild-type (Ly5.1⁺) and *BMPR1 α ^{TR-}* (Ly5.2⁺) mice, along with naive (CD44^{low}CD62L^{high}Ly5.1^{+/-}) CD4⁺ T cells from wild-type mice. 10^5 CD4⁺Foxp3^{GFP} T cells from either *BMPR1 α ^{TR-}* or wild-type mice were co-transferred along with 1.5×10^6 naive T cells from wild-type mice into TCR α ⁻ mice. Mice were monitored for 12 weeks at which time they were sacrificed and mesenteric lymph nodes were isolated and analyzed.

In Vivo Activation and Immunization

For *in vivo* activation, mice were immunized in the footpad with Complete Freund's Adjuvant (CFA; Sigma). Animals were sacrificed 2 weeks later and popliteal draining lymph nodes were isolated and analyzed.

To examine the impact of inflammation on *BMPR1 α* -sufficient and deficient T_{reg} cells mice were infected with *Citrobacter rodentium* to induce mucosal inflammation (Crepin et al., 2016). Mice were analyzed after 8 days.

T Cell Activation

For *in vitro* activation of T_{reg} cells, flow cytometry sorted CD4⁺Foxp3^{GFP⁺} cells were labeled with eFluor 670 (Thermo Fisher Scientific), stimulated with antibodies against CD3 (5 μ g/ml, 2C11; BD Biosciences), with IL-2 (10 ng/ml; PeproTech) and *Haemophilus influenzae* lysate (10 μ g/ml) in the presence of antigen presenting cells in α MEM media (HyClone) supplemented with 10% Fetal Bovine Serum (Atlanta Biologicals), 2 mM L-glutamine, dextrose, essential and non-essential amino acids, sodium pyruvate, sodium bicarbonate, antibiotics, and 2- β -mercaptoethanol. Cells were cultured and analyzed after 3.5 days.

For KDM6B inhibitor studies, flow cytometry sorted CD4⁺Foxp3^{GFP⁺} cells were stimulated with plate-bound antibodies against CD3 (10 μ g/ml, 2C11) and CD28 (1 μ g/ml, 37.51)(both from BD Biosciences), with IL-2 (10 ng/ml; PeproTech) with or without KDM6B inhibitor, GSK-J4 (600 nM; Tocris Bioscience). Cells were cultured and analyzed after 4 days.

To produce polarized effector cells, flow cytometry purified CD4⁺ T cells were stimulated with plate-bound antibodies against CD3 and CD28. For Th17 differentiation, cells were stimulated in the presence of IL-6 (20 ng/ml; PeproTech) and TGF-β (3 ng/ml; PeproTech) in the presence or absence of GSK-J4 (400 nM). For iT_{reg} differentiation, cells were stimulated in the presence of IL-2 (5 ng/ml; PeproTech) and TGF-β (3 ng/ml; PeproTech) in the presence or absence of GSK-J4 (600 nM, Tocris). Cells were cultured and analyzed after 4 days.

For overnight activation, CD4⁺ cells isolated from lymph nodes of TCRα⁻ recipients of adoptively transferred cells were stimulated with Con A (2 μg/ml; Sigma) and analyzed the next day for cytokine production using flow cytometry.

In Vitro T_{reg} Proliferation Inhibition Assay

CD4⁺Foxp3^{GFP-} cells sorted from wild-type mice used as responder cells (5x10⁴/well) were incubated on a 96-well plate with irradiated splenocytes from TCRα⁻ mice (5x10⁴/well, 3000 rad) and soluble anti-CD3ε Ab (5 μg/ml). Various numbers of T_{reg} (CD4⁺Foxp3^{GFP+}) cells (0.5–2.5x10⁴/well) were sorted from wild-type or *BMPR1α*^{TR-} mice and added to responder cells. Proliferation was assessed by measurement of incorporated ³H-thymidine added (1 mCi/well) on the third day of a 4-d culture as described (Kuczma et al., 2009a).

Cell Preparation and Flow Cytometry

Single cell suspensions were prepared from lymph nodes, spleen, thymus or cells activated *in vitro* and stained with antibodies labeled with FITC, PE, PE-Cy5, PE-Cy7, APC, APC-Cy7, Alexa Fluor 680, Alexa Fluor 780, BV421, BV510 or biotin. Antibodies were purchased from eBioscience, BD Biosciences or BioLegend. Following antibodies were used: CD4 (GK1.5), CD8 (53-6.7), CD44 (IM7), CD25 (PC61), CD62L (MEL-14), 4-1BB (17B5), KlrG-1 (2F1), CCR6 (29-2L17), CD127 (A7R34), CD39 (5F2), IL-23R (3C9), CD45.1 (A20) and CD45.2 (104). For intracellular cytokine staining cells were isolated from lymphoid organs or activated *in vitro*. Before staining, cells were incubated for 3 hr. with 10 μg/ml Brefeldin A (BD Biosciences), 50 ng/ml PMA (Sigma) and 1 μg/ml Ionomycin (MP Biomedical) in T cell culture medium. After the 3 hr. incubation period, cells were stained for surface markers first and then fixed using Cytofix/Cytoperm kit (BD Biosciences) and stained with antibodies specific for IFN-γ (XMG1.2), IL-17 (TC11-18H10) labeled with fluorochromes. For intracellular staining for RORC (Q31-378 antibody, BD Biosciences) cells were stained first for surface markers and then for RORC using Transcription Factor Staining Buffer kit (eBioscience). All flow cytometry samples were run on a BD FACSCanto II (BD Bioscience) and analyzed using FlowJo software (Tree Star Inc.). Cell sorting was done on a BD Influx (BD Biosciences). For cell sorting lymph node and spleen cells were enriched by negative selection by staining with biotinylated antibodies specific for CD11b (M1/70), CD11c (HL3), Ter119 (Ter-119), CD49b (DX5) and B220 and magnetic beads (BD IMag, BD Biosciences) selection.

Bromodeoxyuridine Incorporation Assay

For *in vivo* BrdU labeling of proliferating cells, mice were given 0.8 mg/ml BrdU (Sigma) in the drinking water for 4 days. For detection of BrdU incorporation, cells were stained with surface markers and PE-conjugated anti-BrdU antibody according to protocol in BrdU Flow Kit (BD Biosciences). Cells were stained for surface markers first and then fixed using Cytofix/Cytoperm buffer (BD Biosciences) for 30 min. at 4°C. Cells were washed with Cytoperm/Wash buffer, incubated in BD Cytoperm Plus buffer for 10 min. at 4°C, washed again with Cytoperm/Wash buffer and fixed again with Cytofix/Cytoperm buffer for 5 min. After washing with Cytoperm/Wash buffer cells were treated with DNase I (300 μg/ml in PBS, Sigma) for 1 hour at 37°C, washed with Cytoperm/Wash buffer and stained with anti-BrdU antibody for 30 min. at room temp.

Gene Expression Analysis

RNA was prepared according to manufacturer's instructions (PureLink® RNA kit, Thermo Fisher Scientific) and reverse-transcribed with SuperScript IV (Thermo Fisher Scientific) per manufacturer's instructions. Equal amounts of cDNA were used in triplicates to detect transcripts of *BMPR1α* (Mm00477650_m1), *FOXP3* (TaqMan probe set Mm00475157_g1), *KDM6B* (Mm01332680_m1), *RORC* (Mm01261022_m1) and *IL-10* (Mm00439614_m1) using TaqMan® Universal Master Mix II (Thermo Fisher Scientific) in the StepOne Real-Time PCR System (Applied Biosystems). The cycle parameters used were: heating 25 to 50°C for 2 min., 95°C for 10 min., then 40 cycles of 95°C for 15 s. and 60°C for 1 min. The transcript abundance of each gene was normalized to β-actin (TaqMan probe set Mm01205647_g1). Primers for conventional semiquantitative PCR were for *BMPR1α* forward 5'-GCCAGATGATGC TATTAATAACAC, reverse 5'-GGATGCTGCCATCAAAGAACGGAC; β-actin forward 5'-CTAGGCACCAGGGTGTGATGGT, reverse 5'-CTCTTTGATGTCACGCACGATTTT (Table S4) (Kuczma et al., 2014). PCR reaction was done in Mastercycler Plus (Eppendorf) using GoTaq polymerase (Promega). Cycle parameters were: denaturation for 2 min at 94°C and then 30 cycles of 94°C for 10 s., 56°C for 30 s. and 72°C for 45 s.

NanoString Analysis

Multiplex gene expression analysis using an immunology panel of genes was performed by NanoString Technologies. CD4⁺Foxp3^{GFP^{high}} and CD4⁺Foxp3^{GFP^{low}} T cells from *BMPR1α*^{TR-} mice and CD4⁺Foxp3^{GFP} from wild-type mice were flow sorted from lymph nodes and spleens of old (> 7 month) or young (2-3 months) mice. Total RNA was prepared according to manufacturer's instructions (PureLink® RNA kit, Thermo Fisher Scientific). RNA concentrations were determined using a NanoDrop 2000 Spectrophotometer (Thermo Fisher

Scientific). Gene expression analysis was done using Mouse Inflammation Code Set Ver. 2 by NanoString Technologies. Differential gene expression analysis was performed using nSolver software suit. The list of genes differentially expressed between Foxp3^{GFP^{high}} and Foxp3^{GFP^{low}} and wild-type Foxp3^{GFP⁺} T_{reg} cells is included in [Table S1](#) in Supplemental data.

RNA-Seq and Transcriptome Analysis

Global analysis of gene expression was performed using HiSeq 2500 platform in Georgia Cancer Center Core Facility, Augusta University. Naive CD4⁺CD44⁻CD62L⁺Foxp3^{GFP⁻} cells were flow sorted from lymph node and spleens of unmanipulated wild-type mice. Lymph node and spleen cells isolated from wild-type or *BMPR1α*^{T⁻} mice were activated with Con A (2 μg/ml, Sigma) in the presence of IL-2 (5 ng/ml; PeproTech) and TGF-β (3 ng/ml; PeproTech) and activated CD4⁺Foxp3^{GFP⁺} cells were flow cytometry sorted. At least three different samples were processed for each cell type. Total RNA was prepared using commercial kit (QIAGEN). Sequencing library was prepared using Illumina kit. RNA-seq data analysis was performed using Tuxedo protocol as described in ([Trapnell et al., 2012](#)). Briefly, sequencing reads were aligned to reference genome (GRCm38) using Tophat2, followed by estimation of RNA using Cufflinks 2.11. Differential gene expression analysis was performed using Cuffdiff application of Cufflinks. Genes were considered differentially expressed if absolute fold change was greater than 1.5 and adjusted p value was < 0.05. The list of genes is included in [Table S2](#). To visualize differences between gene expression profiles of wild-type and *BMPR1α*-deficient iT_{reg} cells we performed principal component analysis (PCA). The gene lists subject to PCA analysis included all genes with expression levels above the threshold allowing for differential expression analysis in Cufflinks suite. Expression profiles of genes differentially expressed between wild-type and *BMPR1α*-deficient iT_{reg} cells were visualized as volcano plot. Gene Ontology and gene enrichment analyses were performed using Metascape (<http://metascape.org>) ([Zhou et al., 2019](#)). Weighted gene co-expression networks (WGCNA) were generated for populations of wild-type and *BMPR1α*-deficient iT_{reg} cells and activated CD4⁺ T cells using WGCNA package in R ([Langfelder and Horvath, 2008](#)). Expression data for *BMPR1α*-sufficient and deficient naive and activated CD4⁺ T cells were previously published ([Browning et al., 2018](#)). Bioinformatics analyses were performed in College of Public Health of Ohio State University. Networks and network graphs were edited using Cytoscape ([Shannon et al., 2003](#); [Tripathi et al., 2015](#)).

Chromatin Immunoprecipitation (ChIP)

T_{reg} (CD4⁺Foxp3^{GFP⁺}) cells were flow sorted from 3-4 month old wild-type or *BMPR1α*^{TR⁻} mice. ChIP was performed using reagents and protocol from EZ-Chip kit (Millipore). Cells were crosslinked in culture media with formaldehyde (1%) for 10 min. at room temperature. After rinsing with ice-cold PBS cells were lysed in lysis buffer in the presence of protease inhibitors. Cell lysate was sonicated with cup horn sonifier (Branson) on wet ice. An aliquot of lysate was saved as input control at this step. After pre-clearing with protein G agarose beads cell lysates were incubated with anti-H3K27me3 specific antibody (Cell Signaling) overnight at 4°C and immunoprecipitated with protein G agarose. After washing and elution, cross-links were reversed at 65°C for 4 hours. The eluted DNA was purified and samples were analyzed by quantitative-PCR with SYBRGreen using 7900HT real-time PCR cycler (Applied Biosystems). The Ct value for each immunoprecipitated sample was normalized to the corresponding control input value and expressed as fold change relative to control. Primers spanning promoter and control regions of *CDKN1A*, *FOXP3* and *RORC* were as described ([Table S4](#)) ([Ghoreschi et al., 2010](#); [Ishimura et al., 2012](#); [Xiong et al., 2012](#)). Primer sequences are: *CDKN1A* forward 5'-GCACTGGATTGAGACCAGAATC, reverse 5'-CCAAATAGGTCACTGTGCCG and forward 5'-GTTTCAGAGAGGACACTCAGGC, reverse 5'-CTTGATCTCCACGCCAAAG; *FOXP3* forward 5'-ATATTGTTCTGACAGGACTAG, reverse 5'-GCAGCTCAGTGCCA;GAGTGCTTG and forward 5'-CTCTGGAGACAGAGCACTAC, reverse 5'-ACGTTGGAGGATCGCTGGGTT; *RORC* forward 5'-AGAAAGAAAAGGGGAAGTGG, reverse 5'-CTATTGTGGCTGCTGAGTTC. The cycle parameters used were: heating 25 to 50°C for 2 min., 95°C for 10 min., then 40 cycles of 95°C for 15 s., 70°C for 30 s. and 72°C for 30 s.

QUANTIFICATION AND STATISTICAL ANALYSIS

P values were calculated with the two-tailed Student's test for two-group comparison, as applicable, with Microsoft Excel Software. Data are presented as means ± SD. * p < 0.05, ** p < 0.01, *** p < 0.001, **** p < 0.0001, as determined by Student's t test. Network analysis was done using WGCNA and R software.